Rational Synthesis of Unidimensional Mixed Valence Solids. Structural, Spectral, and Electrical Studies of Charge Distribution and Transport in Partially Oxidized Nickel and Palladium Bisdiphenylglyoximates

Martin Cowie,[1a] Alain Gleizes,[1a] Gregory W. Grynkewich,[1a] Davida Webster Kalina,[1a] Malcolm S. McClure,[1b] Raymond P. Scaringe,[1a] Robert C. Teitelbaum,[1a,d] Stanley L. Ruby,[1c] James A. Ibers,*[1a] Carl R. Kannewurf,*[1b] and Tobin J. Marks*[1a,2]

Contribution from the Department of Chemistry, The Department of Electrical Engineering, and the Materials Research Center, Northwestern University, Evanston, Illinois 60201, and the Physics Division, Argonne National Laboratory, Argonne, Illinois 60439. *Received August 23, 1978*

Abstract: This paper presents a detailed study of solid-state structure, oxidation state, and electron transport in $Ni(dpg)_2I$ and $Pd(dpg)_2I$, dpg = diphenylglyoximato. The crystal structure of $Ni(dpg)_2I$ has been studied by X-ray diffraction at 23 and −160 °C. The compound crystallizes from *o*-dichlorobenzene in the tetragonal space group D_{4h}^8-$P4/ncc$, with four formula units of $Ni(dpg)_2I$ in a unit cell having dimensions at −160 °C of a = 19.774 (8), c = 6.446 (3) Å. Full-matrix least-squares refinement of 31 variables gave a final value of the conventional R index (on F) of 0.093 for 353 reflections having $F_o^2 > 3\sigma(F_o^2)$. The crystal structure consists of stacked $Ni(dpg)_2$ units (staggered by 90°) and disordered chains of iodine atoms extending in the c direction. At −160 °C the Ni–Ni separation is 3.223 (2) Å; other important distances are Ni–N = 1.868 (15), N–C = 1.33 (3), N–O = 1.34 (3) Å. The $Ni(dpg)_2$ moiety is decidedly nonplanar (D_2 symmetry) with coordinated N atoms displaced 0.12 (2) Å above or below the mean molecular plane. The form of iodine present, i.e., I_2, I^-, I_3^-, I_5^-, or mixtures thereof, cannot be determined from the Bragg scattering; analysis of diffuse X-ray scattering associated with the disordered iodine chains is consistent with I_5^- being the predominant species. This result is in agreement with resonance Raman spectroscopic studies on $Ni(dpg)_2I$ and $Pd(dpg)_2I$ as well as on an extensive series of selected model compounds. Fundamental polyiodide transitions in the $M(dpg)_2I$ materials are observed (ν_0 = 4880–6471 Å) at 161 vs and 107 w cm^{-1}; weak $M(dpg)_2$-centered scattering is also noted. Iodine-129 Mössbauer data on $Ni(dpg)_2{}^{129}I$ and $Pd(dpg)_2{}^{129}I$ are also in best agreement with the I_5^- formulation. Averaging the data for both compounds, three sites with relative populations 2.04 (10):2.00 (10):1.00 are observed with isomer shifts (vs. ZnTe) = 1.20 (3), 0.52 (5), 0.18 (1) mm/s and e^2qQ = −1764 (5), −1331 (8), −880 (6) MHz, respectively. Thus, the $M(dpg)_2$ units are formally in fractional oxidation states of +0.20 (4). Optical data show transitions at 566 ($Ni(dpg)_2I$) and 505 nm ($Pd(dpg)_2I$) which are most likely associated with the $M(dpg)_2$ stacking interaction, and a broad band in both materials at 675 nm which is assigned to the polyiodide chains. X-ray photoelectron spectra ($Ni2p_{3/2}$, $Pd\ 3d_{3/2}$, $3d_{5/2}$) show no evidence of trapped valence. Single crystal electrical conductivity (both dc and 100-Hz ac) in the c (chain) direction is as high at 30 °C as 1.1×10^{-1} ($Ni(dpg)_2I$) and 4.7×10^{-3} $(\Omega\ cm)^{-1}$ ($Pd(dpg)_2I$). Iodination brings about an increase in conductivity of $>10^8$ (Ni) and $>10^7$ (Pd), which is especially noteworthy since the only major change in crystal structure upon iodination is a ca. 0.27 Å decrease in the $M(dpg)_2$ stacking distance. Variable-temperature studies show the $Ni(dpg)_2I$ and $Pd(dpg)_2I$ conductivities to be thermally activated, with activation energies of 0.19 ± 0.01 and 0.54 ± 0.11 eV, respectively.

Solids with strongly unidimensional structural and electronic interactions have attracted much recent attention among chemists and physicists.[3] New materials with quasi-metallic electrical, optical, and magnetic properties concentrated largely in one (or two) dimension(s) have forced a progressive refinement of theoretical models as well as experimental expectations for cooperative phenomena in molecular solids. The ultimate goal of such research is to develop theory and chemical methodology to the point that such cooperative phenomena can be varied at will.

It has been our interest to explore general approaches to the chemical synthesis of quasi-metallic assemblages composed of molecular stacks or chains, and to employ the physical properties of the resulting designed materials to test current ideas regarding electron-transport phenomena. Judging from what is presently known about highly conductive stacked systems such as KCP [$K_2Pt(CN)_4Br_{0.30}\cdot 3H_2O$] and TTF-TCNQ, as well as systems which, in contrast, do not undergo a low-temperature transition to the semiconducting state,[3,4] it is reasonable to attempt to array, in close proximity, flat, highly delocalized, polarizable molecules.[3,5] It is assumed, of course, that the stacked components occupy sites which are crystallographically as similar as possible. A crucial feature which also appears to be inextricably connected with facile electron transport, and which is understandable within the framework of the one-dimensional Hubbard band model,[3] is mixed valency.[3,6] That is, the molecular units to be connected in series must have fractional formal oxidation states. One plausible approach[7a] which we have investigated to ensure mixed valency has been to attempt to cocrystallize stacks of planar donor molecules, D, with an array of suitable acceptor

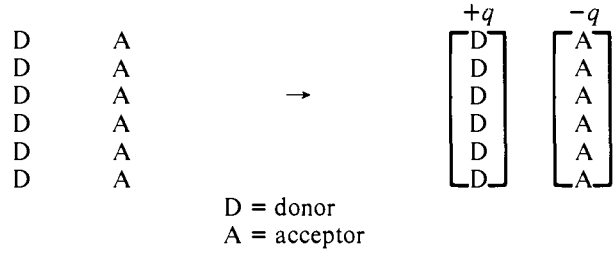

species, A, which would each remove a nonintegral amount of electronic charge per D unit ("partial oxidation"). The A moieties should be polarizable and must be sufficiently compact to pack easily within the assembly of D_n stacks. To promote mixed valency A must form stable polynuclear anions, A_n^{-1}.[7a] Thus, in the hypothetical material $DA_{1.0}$, each A would increase the formal oxidation state of each D by $+1/n$.

Our efforts to synthesize mixed-valence structures by the above strategy have so far focused primarily on the use of iodine as an acceptor.[7,8] Polyiodides such as I_3^- and I_5^- exhibit

0002-7863/79/1501-2921$01.00/0

high thermodynamic stability in nonpolar media similar to environments expected in many D_n lattices and possess shapes which should not drastically restrict the formation of one-dimensional arrays.[9] Furthermore, iodine-containing oxidants are readily amenable to characterization by the powerful combination of resonance Raman and iodine-129 Mössbauer spectroscopy.[7,10] Thus, in a material of stoichiometry DI, identifying the iodine as I_2, I^-, I_3^-, I_5^-, or a combination thereof allows a direct and accurate estimation of the electronic charge transferred from D to the acceptor. Such charge distribution information is of great importance in formulating models for electron transport and is not readily available for noncrystalline, microcrystalline, or severely disordered materials.[3]

The earliest recognized examples of stacked, square-planar metal complexes were the bisglyoximates of nickel, palladium, and platinum, A.[11] It has been known for some time that the

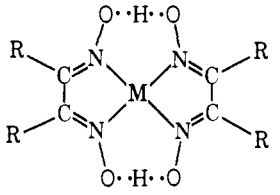

A

R = CH_3: M(dmg)$_2$

R = C_6H_5: M(dpg)$_2$

M = Ni, Pd, Pt

nickel and palladium bisdiphenylglyoximates can be reversibly iodinated (or brominated), as illustrated in the equation[12]

$$M(dpg)_2 + \tfrac{1}{2}I_2 \rightleftharpoons M(dpg)_2I \qquad (1)$$

M = Ni,Pd

The products are lustrous, golden-olive needles which exhibit weak, temperature-independent paramagnetism and pressed pellet electrical conductivities which are ca. 10^4 greater than in the unhalogenated materials.[13] Subsequent studies have inferred the basic one-dimensional nature of the M(dpg)$_2$I crystal structure and have thoroughly categorized the range of stoichiometries and halogenation products which exist.[14] However, this information did not resolve the fundamental question of whether these materials were or were not mixed valent, and the form of the iodine was variously formulated in the past as I_2 (formally Ni^{2+}, a halogen charge-transfer complex[15]), I^- (formally Ni^{3+}),[16] and I_3^- (formally $Ni^{2.33+}$, partially oxidized).[14c] Thus, it was of great interest to us to investigate the M(dpg)$_2$I systems in greater detail as the first prototypes of mixed valence lattices synthesized via the polyiodide strategy. In our initial communications on this subject[7c,d] we showed on the basis of preliminary spectral and diffraction data that the presence of significant amounts of I_2 or I^- in the M(dpg)$_2$I materials could be clearly rejected. In this paper we present a full exposition of our structural, spectral, and electron-transport measurements on the nickel and palladium bisdiphenylglyoximato iodides. It is unequivocally demonstrated that these systems do contain M(dpg)$_2$ units in formal fractional oxidation states, and that the spectral methods for charge distribution analysis have wide applicability. In so doing we modify, on the basis of improved spectroscopic and diffraction data, our original suggestion[7c,d] that the iodine-containing species is largely I_3^- in these systems; rather we show that it is largely if not exclusively I_5^-. In a companion paper[7b] we examine the structural and electronic characteristics of the more closely coupled and highly conjugated nickel and palladium bisbenzoquinonedioximato iodides, which provide further insight into the response of stacked metal dioximate systems to partial oxidation.

Experimental Section

Elemental analyses were performed by Ms. H. Beck, Northwestern Analytical Services Laboratory, or Micro-Tech Laboratories. All halogenated samples were stored in closed vials in a freezer at −20 °C in the dark.

Synthesis of M(dpg)$_2$I Compounds, M = Ni, Pd. Bis(diphenylglyoximato)nickel(II) was prepared by reaction of diphenylglyoxime (Eastman) with $NiCl_2 \cdot 6H_2O$ in refluxing ammoniacal ethanol.[14a] Bis(diphenylglyoximato)palladium(II) was prepared in a similar manner using $PdCl_2$.[14b] Both complexes were purified by several recrystallizations from hot dimethylformamide. The corresponding iodides were prepared by reacting *o*-dichlorobenzene solutions of the metal diphenylglyoximates (ca. 10^{-3} M) at 110 °C with a ca. 35–150-fold molar excess of triply sublimed I_2. The hot solution was gravity filtered, rewarmed to 110 °C, and then slowly cooled to room temperature in an insulated Dewar flask over a period of 3–5 days. The golden-olive crystals obtained were collected by suction filtration and were washed with pentane until the washings were colorless. Yields by this procedure ranged from 40 to 60%.

Anal. Calcd. for Ni($C_{14}H_{11}O_2N_2$)$_2$I: C, 50.63; H, 3.34; N, 8.44; I, 19.11. Found: C, 50.92; H, 3.10; N, 8.39; I, 19.37. Calcd for Pd($C_{14}H_{11}O_2N_2$)$_2$I: C, 47.24; H, 3.12; N, 7.87; I, 17.83. Found: C, 47.04; H, 3.13; N, 7.75; I, 17.30.

Complete infrared spectra (Nujol mulls, cm^{-1}) follow.

Ni(dpg)$_2$: 3090 vw, 3075 w, 3060 mw, 1985 vw, 1965 vw, 1895 vw, 1805 vw, 1765 vw, 1600 vw, 1580 mw, 1530 vs, 1490 vs, 1445 vs, 1320 w, 1290 s, 1210 m, 1155 mw, 1140 vw, 1070 m, 1000 mw, 970 m, 930 ms, 900 s, 850 m, 810 m, 775 ms, 740 vs, 690 vs, 670 w, 384 w, 323 vs, 295 s, 248 w, 176 vs, 130–140 m.

Ni(dpg)$_2$I: 3075 w, 1965 vw, 1820 vs, 1600 mw, 1580 w, 1530 m, 1490 s, 1445 vs, 1330 m, 1295 s, 1280 ms, 1220 w, 1155 mw, 1140 vs, 1070 mw, 1025 w, 975 mw, 930 ms, 900 s, 850 mw, 820 w, 770 s, 740 s, 690 vs, 670 mw, 388 m, 365 vs, 319 s, 298 vs, 260 w, 174 vs, 130–140 s.

Pd(dpg)$_2$: 3090 vs, 3070 w, 3060 mw, 1985 vw, 1965 vw, 1895 vs, 1810 vw, 1765 vw, 1600 vs, 1580 mw, 1520 m, 1490 s, 1445 vs, 1340 mw, 1325 m, 1300 s, 1280 m, 1190 mw, 1160 ms, 1140 mw, 1070 m, 1025 ms, 1000 m, 970 ms, 930 m, 885 s, 840 mw, 815 mw, 760 mw, 740 vw, 690 vs.

Pd(dpg)$_2$I: 3070 w, 1975 vw, 1900 vw, 1820 vw, 1590 mw, 1570 mw, 1510 mw, 1485 m, 1440 vs, 1345 m, 1335 m, 1305 s, 1280 m, 1155 m, 1135 m, 1070 mw, 1025 m, 1000 w, 970 mw, 920 mw, 880 s, 845 w, 810 w, 765 s, 740 vs, 690 vs.

The above synthetic procedure was found consistently to produce the largest M(dpg)$_2$I crystals; however, overall yields were diminished somewhat. Larger yields of the M(dpg)$_2$I materials can be obtained by using more concentrated solutions, but more rapid crystallization and smaller crystals result. With a deficiency of iodine, dilute or concentrated solutions yield products which, by optical microscopy, are seen to be mixtures of light- and dark-colored crystals. Mechanical separation and elemental analysis show these to be the M(dpg)$_2$ and M(dpg)$_2$I$_{1.0}$ derivatives, respectively.

Synthesis of M(dpg)$_2$^{129}I Compounds, M = Ni, Pd. For the Ni(dpg)$_2$^{129}I and Pd(dpg)$_2$^{129}I Mössbauer samples, the above procedure was carried out on a smaller scale using more concentrated *o*-dichlorobenzene solutions and a ca. 7 molar excess of $^{129}I_2$. The latter reagent was prepared by oxidizing acidified Na^{129}I solutions (Oak Ridge National Laboratory) with 30% H_2O_2 and extracting the iodine into *o*-dichlorobenzene. The organic layer was next separated, washed twice with distilled water, and dried over anhydrous Na_2SO_4. This solution was then used for M(dpg)$_2$ iodination.

Synthesis of M(dpg)$_2$Br Compounds, M = Ni, Pd. The compounds Ni(dpg)$_2$Br and Pd(dpg)$_2$Br were prepared by reacting the M(dpg)$_2$ compounds in CCl_4 with Br_2 as described by Edelman.[12] These compounds lose halogen at room temperature far more rapidly than do the iodides.

Complete infrared spectra (Nujol mulls, cm^{-1}) follow.

Ni(dpg)$_2$Br: 3075 w, 1970 vw, 1820 vw, 1600 mw, 1575 w, 1525 mw, 1490 s, 1445 vs, 1330 m, 1295 s, 1280 ms, 1155 m, 1140 vs, 1100 mw, 1070 mw, 1025 w, 1000 w, 975 mw, 930 m, 900 ms, 850 w, 770 s, 740 s, 690 vs, 670 mw, 388 m, 363 s, 320 ms, 298 s, 261 w, 173 vs, 110–140 s.

Pd(dpg)$_2$Br: 3075 w, 1970 vw, 1820 vw, 1595 mw, 1575 w, 1515 w, 1485 m, 1440 vs, 1335 m, 1300 s, 1275 m, 1150 m, 1140 m, 1070 w, 1025 m, 1000 w, 975 w, 925 mw, 880 s, 840 vw, 805 vw, 775 w, 765 s, 740 vs, 690 vs.

Raman Measurements. Laser Raman spectra were recorded with Kr^+ (6471 Å) or Ar^+ (4880, 5145 Å) excitation using a Spex 1401 monochromator and photon counting detection. The solid samples were studied in 5- or 12-mm Pyrex sample tubes spinning at 1200 rpm. A 180° backscattering geometry was employed. A number of scans were made of each sample (the initial at lowest laser power) to check for possible sample decomposition. Spectra were calibrated with the exciting line (ν_0) or laser plasma lines. For variable-temperature studies the spinning sample was placed in a transparent glass Dewar and was cooled in a stream of boil-off nitrogen. Temperatures were calibrated with a copper-constantan thermocouple. Spectra at ca. 8 K were obtained using an apparatus described elsewhere.[17]

Infrared Measurements. Routine infrared spectra were recorded with a Perkin-Elmer Model 267 spectrophotometer. Far-infrared spectra were obtained with a Perkin-Elmer Model 180 instrument. Samples were studied as Nujol mulls between KBr or polyethylene plates. The far-infrared studies were performed with a thorough and continuous purge of dry nitrogen.

Iodine-129 Mössbauer Spectroscopy. For Mössbauer measurements, source, absorber, and detector were employed in the standard transmission geometry. The $^{66}Zn^{129}Te$ source ($t_{1/2}$ = 69 min) was prepared by irradiation of a $^{66}Zn^{128}Te$ target (pressed in an aluminum disk) in the Argonne CP-5 reactor for 2 h. The source produced sufficient 27.7-keV γ-radiation for 3–4 h of Mössbauer effect data collection. Absorbers were prepared by powdering the iodine-129 enriched samples, mixing with an inert filler (boron nitride), and loading into Lucite sample holders. The absorbers typically contained ca. 7 mg $^{129}I/cm^2$, which represents a compromise between large Mössbauer effect γ-ray absorption, self-absorption, Compton scattering, and thickness errors. Both the source and absorber were cooled to 4.2 K during data collection. Typically, three or four sources were used, in sequence, to collect all the data for a given sample. Data collected from each source were summed to give the final spectra. Individual runs were checked for reproducibility. Attempts to observe spectra with the sample at 77 K were unsuccessful, owing to the low ^{129}I recoilless fraction. The spectrometer velocity was generated with a feedback-controlled vibrator using sinusoidal acceleration. The velocity drive was calibrated with ^{57}Fe foil. Data were collected with a proportional counter in conjunction with a 400-channel multichannel analyzer operating in the time mode. Data were stored on paper tape.

Mössbauer effect data processing and analysis employed the computer program GENFIT,[18] which finds the best values of the parameters of isomer shift, quadrupole coupling constant, line width, populations, base line, and asymmetry parameter via nonlinear least-squares minimization of the difference between the observed and calculated spectra. The goodness of fit is judged by the parameter "Misfit," which has been previously defined by Ruby.[19a] "Misfit", which is a modification of the parameter χ^2,[19b] is better suited to deciding which of several modes fits several measurements more accurately.

The end sites in the pentaiodide ion showed large line widths in comparison with the other iodine sites. This could be explained if the end sites have a distribution of quadrupole coupling constants. That is, not all end sites are exactly equivalent. This nonequivalence was incorporated in the fitting procedure as a velocity-dependent line-broadening function:

$$\Gamma_n = \sqrt{[\kappa(V_n - \delta)]^2 + \Gamma_{true}^2} \qquad (2)$$

where Γ_{true} is the actual line width, δ is the isomer shift, V_n is the velocity of line n, κ is the broadening parameter, and Γ_n is the observed width of the nth line. This function broadens the lines furthest away from the center of gravity (δ, isomer shift) to a greater extent than those lines closer to δ. This has the same overall effect as a quadrupole distribution. Using this value of Γ_n, reasonable line widths for all sites are obtained.

Electronic Spectra. Spectra of solid samples were studied as Nujol mulls between quartz plates in a Cary 17-D spectrophotometer. Several scans were made of each sample to check for possible decomposition.

Single Crystal Conductivity Measurements. Samples selected for electrical conductivity measurements had no apparent growth defects that could be observed by microscopic inspection. Typical sample dimensions for the tetragonal needles were 2.0–3.0 mm in length and 0.1–0.2 mm in thickness. All measurements were performed with current flow along the c-axis direction.

Mounting and electrode attachment employed the conventional four-probe technique. The substrate mounts were prepared from a typical integrated circuit header assembly before encapsulation. Small-diameter gold or aluminum wires served as electrode connectors and were attached to the samples using either colloidal graphite suspended in 1,3-butylene glycol or Demetron M8001 cold-setting conductive gold contact paint. Conductivity results with these two contact materials were identical. In addition, it was found that conductivities remained constant over a period of days at room temperature, indicating that no reaction was taking place between sample and contact material. Sample electrode arrangements were checked by the procedure of Schafer et al.[20]

Current for dc conductivity measurements was supplied by a Keithley Model 225 regulated current source; voltage was measured by two Keithley Model 610 B electrometers in differential configuration. Several low-frequency ac (100 Hz) measurements were performed using PAR 124 and HR8 lock-in amplifiers. The results were in good agreement with the dc measurements. Variable-temperature studies were conducted in a Delta Design environmental chamber. Temperatures were monitored with a copper-constantan thermocouple adjacent to the sample. Room temperature measurements were always made after high-temperature (>300 K) studies to check for possible sample decomposition.

X-ray Photoelectron Spectroscopy. XPS spectra were recorded on an AEI-ES100B spectrometer using Al Kα radiation. Time averaging was performed with a PDP-8S data system. A least-squares fit of the data points was achieved using the program SMOOTH II.[21] Spectra were recorded at room temperature. In order to check for possible loss of iodine from the $M(dpg)_2I$ compounds in the high vacuum of the spectrometer, the I $3d_{5/2}$ peak was recorded at the beginning and end of each run; no drop in the intensity of this peak was observed. Furthermore, spectra recorded at −50 °C were identical with those obtained at room temperature. Attempts at argon ion etching did, however, result in loss of iodine from the $M(dpg)_2I$ complexes and apparent reduction to $M(dpg)_2$ (even at low temperature). Binding energies reported are relative to C 1s (taken to be 285.0 eV). The uncertainty in these numbers is somewhat large owing to the rather large shift (0.3–0.9 eV) in C 1s kinetic energy observed in the course of the runs (a period of several hours), most likely a consequence of charging effects. An attempt was made to obtain the relative binding energies of $M(dpg)_2I$ vs. $M(dpg)_2$ by running a homogeneously mixed sample of the two materials. In each case, no splitting or broadening of the peaks was observed.

X-ray Diffraction Study of $Ni(dpg)_2I$. Crystals of $Ni(dpg)_2I$, suitable for X-ray diffraction studies, were grown by the slow cooling of *o*-dichlorobenzene solutions containing an excess of iodine as described above. The crystals obtained are black, very thin needles with a silver, metallic luster. The crystal structure of $Ni(dpg)_2I$, based on diffractometer data collected at room temperature, has been described.[7c,d] In an attempt to characterize more fully the nature of the iodine-containing species, a low-temperature study has been carried out.

For the low-temperature study a suitable, although rather small, crystal was mounted with G.E. Glyptal to a copper fiber (diameter = 0.5 mm) in an Air Products Cryo-tip goniometer equipped with a closed Joule-Thomson cooling cycle. The crystals have the same space group at both 23 and −160 °C. Accurate cell parameters at −160 (5) °C were obtained by a least-squares analysis of the setting angles of 13 hand-centered reflections chosen from diverse regions of reciprocal space (29.0° ≤ 2θ ≤ 57.1°, Cu Kα_1 radiation) and obtained using a narrow X-ray source. Table I contains pertinent crystal data for the low-temperature study.

The low-temperature data were collected on a Picker four-circle automated diffractometer as has previously been described.[22] The intensities of six standard reflections were measured every 100 reflections to assess crystal movement or decomposition. There was no significant variation in these standards. The intensities of 1102 accessible reflections with indices $l \geq 0$ and $h \geq k \geq 0$ were measured for 2° ≤ 2θ ≤ 120° using nickel-filtered Cu Kα radiation. Of these, 416 have $F_o^2 \geq 3\sigma(F_o^2)$. The data were processed in the usual way using a value of 0.04 for p.[23] An absorption correction was applied to the data using Gaussian integration.[24]

Structure Solution and Refinement. The positions of all nonhydrogen atoms were taken from the room temperature determination,[7c] with the nickel atoms on the 4(a) special positions and the iodine atoms on the 4(c) special positions in space group $P4/ncc$ (with unit cell origin at $\bar{1}$). The structure was refined using full-matrix, least-squares techniques, minimizing the function $\Sigma w(|F_o| - |F_c|)^2$, where $|F_o|$

Table I. Summary of Crystal Data, Intensity Data Collection, and Refinement for $Ni(dpg)_2I$ at −160 °C

temp	−160 (5) °C
formula	$C_{28}H_{22}IN_4NiO_4$
formula weight	664.1 amu
space group	D_{4h}^8-$P4/ncc$
a	19.774 (8) Å[a]
c	6.446 (3) Å
V	2520 Å^3
Z	4
density	1.750 g/cm^3 (calcd)
crystal dimensions	0.53 × 0.04 × 0.04 mm
crystal shape	needle with well-developed faces of the forms {001}, {100}, and {110}. [001] is the needle direction
crystal volume	0.000 51 mm^3
radiation	Cu Kα_1 (1.540 562 Å)
μ	111.8 cm^{-1}
transmission factors	0.615–0.731
receiving aperture	4.1 × 4.1 mm, 32 cm from crystal
take-off angle	3.1°
scan speed	1°/min
scan range	0.9° below Kα_1 to 0.9° above Kα_2
background counts	40 s
2θ limits	2.0–120.0°
final no. of variables	31
unique data used	353
error in observation of unit weight	4.03 electrons
R	0.093
R_w	0.126

[a] The cell parameters at 23 (1) °C are a = 19.887 (4) Å, c = 6.542 (2) Å, and V = 2587 Å^3.

and $|F_c|$ are the observed and calculated structure amplitudes and the weights, w, are taken as $4F_o^2/\sigma^2(F_o^2)$. The agreement indices are defined as $R = \Sigma||F_o| - |F_c||/\Sigma|F_o|$ and $R_w = [\Sigma w(|F_o| - |F_c|)^2/\Sigma wF_o^2]^{1/2}$. Atomic scattering factors were taken from the usual sources.[25] Anomalous dispersion terms[26] for the Ni and I atoms were included in F_c. A series of θ–2θ scans performed for $2° \le 2\theta \le 110°$ in several arbitrary crystal orientations indicated the regions of interference from the Cu powder pattern of the Cu fiber. These regions agree well with those calculated for copper scattering at −160 °C. Owing to the low intensities of many reflections, these powder lines constitute a significant contribution to the observed intensities so all data in these regions of 2θ were eliminated from further refinements, leaving 353 reflections with $F_o^2 \ge 3\sigma(F_o^2)$. Although a difference Fourier synthesis enabled us to locate all the hydrogen atoms, their positions were idealized. A C–H distance of 0.95 Å was assumed for the hydrogen atoms of the phenyl groups. The hydrogen atom of the hydroxyl group was placed on the crystallographic twofold axis between the two oxygen atoms. Each hydrogen atom was assigned a thermal parameter of 1 Å^2 greater than that of the atom to which it is attached.

In the low-temperature structure all thermal parameters are, as expected, significantly lower than those at room temperature. However, as was found earlier,[7c] the mean-square amplitude of vibration of the I atom in the c direction (U_{33}) is approximately ten times greater than it is normal to this direction.

For reasons to be discussed later, it is certain that the apparent high thermal motion of the iodine atoms is caused by a disorder in the iodine chain. Hence, there is a distribution of possible iodine atom positions in the cell. Under these circumstances the use of thermal parameters will not reproduce the observed electron density distribution unless one of the following is true:[27] (1) The magnitude of the displacements characteristic of the disorder is small. (2) The distribution of displacements (whether or not their magnitudes are small) is Gaussian. Since in the present case neither of these conditions applies, several peaks in the difference Fourier map persisted throughout anisotropic refinement. The optimal solution to this problem would involve proposing a detailed model for the disorder and then reproducing the predicted electron density distribution by placing atoms with fractional occupancy factors in appropriate positions. However, to arrive at such a model based on the structureless mass of electron density along the line $\frac{1}{4}$, $\frac{1}{4}$, z is obviously out of the question. In theory, a detailed disorder model can be deduced by interpretation of the diffuse scattering; efforts are being made in this direction and will be discussed later. An alternative approach is to approximate the observed electron density distribution by some function other than the Gaussian. We have applied this idea successfully to a similar structure,[28] but in the present case we have been unable to find a distribution which yields results superior to those for the Gaussian.

In the final least-squares refinement only one I atom position was refined and the solution converged to values of R and R_w of 0.093 and 0.126, based on 31 variables and 353 observations. The error in an observation of unit weight is 4.03 electrons. An analysis of $\Sigma w(|F_o| - |F_c|)^2$ as a function of F_o, setting angles, and Miller indices shows no unusual trends apart from the poor agreement at low θ values. This is to be expected on the basis of the I-atom disorder. The highest 15 peaks in a final difference Fourier synthesis are between the I atoms in the I chains (3.5–3.6 (1) e Å^{-3}), between the Ni atoms (1.3–1.5 (2) e Å^{-3}), near the oxygen atoms (0.9–1.0 (2) e Å^{-3}), and near the phenyl rings (0.7 (2) e Å^{-3}). The residuals between the I and Ni atoms are probably a consequence of the disorder of the I atoms and the resulting poor refinement of the ordered model, although electron density errors are expected to be higher in special positions.

The final positional and thermal parameters appear in Tables II and III. Root mean square amplitudes of vibration of the I and Ni atoms at both 23 and −160 °C are given in Table IV. A listing of the observed and calculated structure amplitudes is available.[29]

Diffuse X-ray Scattering. Examination of ordinary oscillation photographs taken with nickel-filtered Cu radiation revealed the presence of three weak layers at ca. 2.12, 2.44, and 2.80 reciprocal lattice units in addition to the normal Bragg layer lines. Subsequent stationary crystal photographs demonstrated that the extra scattering is concentrated in planes normal to the c axis. These observations clearly indicate the existence of one-dimensional disorder in this material. We identify the disorder with the iodine chain because of the apparent high thermal motion of the iodine atoms and because the resulting model (I^- ion separated by ~3.26 Å) is physically unrealistic. The intensity in any given diffuse layer is slightly modulated indicating that some three-dimensional correlations are present between chains. Diffuse scattering similar to that observed here is well documented for materials containing iodine chains.[7a,8c,30] In these cases, the diffuse layers can be indexed on the basis of a 9.7-Å superlattice and the interpretation of intensity data, when measured, yields disorder models

Table II. Positional and Thermal Parameters for the Nongroup Atoms of Bis(diphenylglyoximato)nickel Iodide

ATOM	x[A]	y	z	B11[B] OR B,Å^2	B22	B33	B12	B13	B23
I	1/4	1/4	0.02421121	0.99(6)	0.99	102.13)	0	0	0
NI	-1/4	1/4	-1/4	0.79(10)	0.79	2.41191	-0.18(27)	0	0
N	-0.1560(8)	0.2572(10)	-0.2314(28)	0.9(3)					
O	-0.1164(9)	0.2021(9)	-0.238(3)	2.7(4)					
C	-0.1289(10)	0.3186(11)	-0.201(4)	0.3(5)					
H	-0.340	0.340	-1/4	3.7					

[a] Estimated standard deviations in the least significant figure(s) are given in parentheses in this and all subsequent tables. [b] The form of the anisotropic thermal ellipsoid is: $\exp[-(B11h^2 + B22l^2 + B33k^2 + 2B12hk + 2B13hl + 2B23kl)]$. The quantities given in the table are the thermal coefficients × 10^3.

Table III. Derived Parameters for the Rigid Group Atoms of Bis(diphenylglyoximato)nickel Iodide

ATOM	X	Y	Z	B,A^2	ATOM	X	Y	Z	B,A^2
C(1)	-0.0584(6)	0.3341(8)	-0.3081(26)	1.2(5)	H(2)	-0.016	0.260	-0.129	2.3
C(2)	-0.0064(7)	0.2949(7)	-0.2262(23)	1.3(5)	H(3)	0.096	0.280	-0.230	2.2
C(3)	0.0612(6)	0.3066(8)	-0.2863(27)	1.2(5)	H(4)	0.120	0.366	-0.469	4.7
C(4)	0.0747(6)	0.3576(9)	-0.4284(28)	3.8(8)	H(5)	0.033	0.432	-0.607	2.4
C(5)	0.0227(8)	0.3968(7)	-0.5103(24)	1.4(5)	H(6)	-0.079	0.412	-0.506	2.0
C(6)	-0.0438(7)	0.3850(7)	-0.4501(25)	1.0(5)					

RIGID GROUP PARAMETERS

GROUP	x_c[A]	y_c	z_c	DELTA[B]	EPSILON	ETA
C-RING	0.0082(5)	0.3458(5)	-0.3682(17)	-2.748(11)	-2.499(10)	-2.787(13)
H-RING	0.0082	0.3458	-0.3682	-2.7481	-2.4998	-2.7864

[a] x_c, y_c, and z_c are the fractional coordinates of the origin of the rigid group. [b] The rigid group orientation angles delta, epsilon, and eta (radians) have been defined previously: S. J. La Placa and J. A. Ibers, *Acta Crystallogr.*, **1965**, *18*, 511-519.

Table IV. Root Mean Square Amplitudes of Vibration (Å) of $Ni(dpg)_2I$ at 23 and −160 °C

atom	temp, °C	min	intermediate	max
I	23	0.234 (4)	0.234	0.756 (11)
Ni	23	0.13 (2)	0.17 (2)	0.21 (2)
I	−160	0.140 (4)	0.140	0.462 (8)
Ni	−160	0.07 (3)	0.11 (3)	0.14 (2)

involving the triiodide ion as the iodine-containing species. In the present case this interpretation is not possible. In $Ni(dpg)_2I$, counter measurements of the diffuse scattering pattern employing monochromatic Co Kα (λ = 1.7889 Å) radiation indicate irregular layer spacings and broadening, suggestive of a system displaying short-range order. An experimental example of this phenomenon has been reported for the one-dimensional material hollandite.[31] We are currently analyzing the diffuse scattering pattern of $Ni(dpg)_2I$ in terms of short-range order models. Although optimization of the model is not yet complete, the agreement with experiment at present is sufficiently close that qualitative information about the iodine species in this material is now available.[28] In particular, all attempts to reproduce the observed scattering in terms of models with I_3^- or I_2 have been unsuccessful. The primary reason for this is that it is difficult, if not impossible, to postulate a sensible physical model based on these species which reproduces the main feature of the observed scattering pattern (the intense peak at 2.06 reciprocal lattice units). This is in agreement with the ^{129}I Mössbauer and resonance Raman results (see Results section) which indicate that these species are either completely absent or present in small amounts only. Of the numerous models considered thus far, only those involving groupings of I_5^- [32] as the predominant species have met with success in explaining the experimental data.

Results and Discussion

Chemistry. The compounds $Ni(dpg)_2I$ and $Pd(dpg)_2I$ were prepared as shown in eq 1. Very slow cooling of hot *o*-dichlorobenzene solutions of the $M(dpg)_2$ complexes with a large excess of iodine produced lustrous, golden-olive crystals of sufficient size for X-ray diffraction and electrical conductivity studies. Under the synthetic conditions employed, the metal:I ratio in the product was consistently found to be 1.00:1.00 ± 0.05. When deficiencies of iodine were employed, the slow cooling technique produced mixtures of $M(dpg)_2$ and $M(dpg)_2I$ crystals, which could be mechanically separated and characterized (see Experimental Section). There was also no evidence from laser Raman spectroscopy (vide infra) that $M(dpg)_2I_x$ materials were present with x not 1.0 or 0.0. Similarly, $M(dpg)_2I$ compounds were found to lose I_2 upon heating, and at no time during this process were Raman signals observed for materials other than x = 1.0 or x = 0.0.

Table V. Selected Distances and Angles in $Ni(dpg)_2I$ at −160 °C

	Bond Distances (Å)		
Ni-N	1.868 (15)	C-C′[a]	1.61 (4)
N-O	1.34 (2)	C-C(1)	1.59 (2)
N-C	1.33 (3)	O-H	1.20
	Nonbonded Contacts (Å)		
I-I	3.223 (2)	C(1)-C(6)′	3.14 (2)
Ni-Ni	3.223 (2)	C(1)-O	2.89 (2)
O-O‴	2.40 (4)	C(2)-O	2.85 (2)
O-H(2)	2.39	C(6)-O	2.91 (2)
C(1)-H(6)′	2.72	C(6)-C	2.91 (3)
C(1)-C(1)′	3.10 (3)	C(6)-C(1)′	3.14 (2)
	Angles (deg)		
N-Ni-N′	81.5 (12)	N-C-C′	105.7 (13)
N-Ni-N‴	99.0 (12)	N-C-C(1)	118.1 (18)
N-Ni-N″	172.7 (11)	C′-C-C(1)	105.9 (16)
Ni-N-O	121.1 (15)	C-C(1)-C(2)	112.0 (14)
Ni-N-C	118.6 (15)	C-C(1)-C(6)	127.7 (13)
	Torsion Angles (deg)		
O-N-N″-O″	−176 (2)	C(1)-C-C′-C(1)′	−75 (2)
O-N-N‴-O‴	2 (2)	C(2)-C(1)-C-C′	175 (2)
N-C-C′-N′	33 (2)	C(2)-C(1)-C-N	−66 (2)

[a] Primed atoms are related by the twofold axes at −¼, ¼, −¼. See Figure 3 for the numbering scheme of the $Ni(dpg)_2^+$ cation.

Crystal Structure of $Ni(dpg)_2I$. The structure of $Ni(dpg)_2I$ consists of discrete $Ni(dpg)_2$ units and I atoms with no unusual nonbonded contacts (see Table V). The $Ni(dpg)_2$ units are stacked along the crystallographic *c* axis with the coordination plane of the Ni atom perpendicular to the stacking direction. Each $Ni(dpg)_2$ unit is staggered by 90° with respect to its nearest neighbor along the stacking axis. The iodine atoms also stack one above the other in the *c* direction, filling the "tunnels" created by the phenyl rings of the diphenylglyoximato ligands. The packing is shown in the stereoscopic view of the unit cell contents in Figure 1. Figure 2 shows stacking of the Ni and I atoms in the *c* direction. A drawing of the $Ni(dpg)_2$ unit showing relevant bond lengths and angles is presented in Figure 3.

The Ni atoms occupy the 4(a) special positions in the space group $P4/ncc$. Therefore, all Ni atoms are equally spaced along the stacking direction by $c/2$ (3.223 (2) Å). This distance can be compared with the corresponding Ni-Ni distances in the stacked compounds $Ni(dpg)_2$ (3.547 Å),[14d] $Ni(dmg)_2$ (3.25 Å),[11] $Ni(bqd)_2I_{0.018}$ (3.180 (2) Å),[7b] were bqd = benzoquinonedioximate, $Ni(bqd)_2I_{0.5}$ (3.153 (3) Å),[33] Ni(Pc) (4.79 Å),[34] where Pc = phthalocyanine, and $Ni(Pc)I_{1.0}$ (3.244 (3)

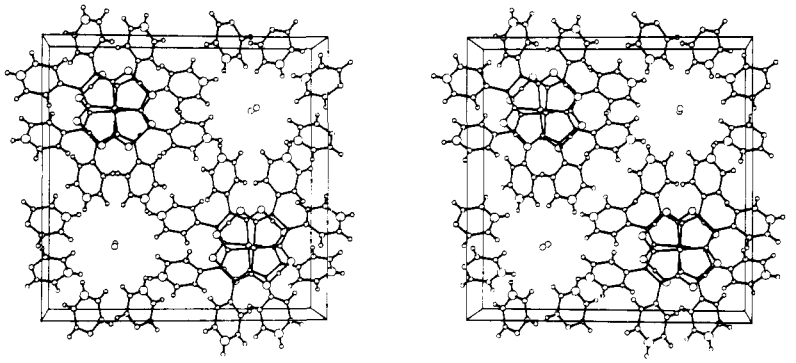

Figure 1. A stereoview of the unit cell of $Ni(dpg)_2I$. The *a* axis is horizontal to the right, the *b* axis is vertical from bottom to top, and the *c* axis is toward the reader. The vibrational ellipsoids are drawn at the 50% level, except hydrogen atoms, which are drawn arbitrarily small.

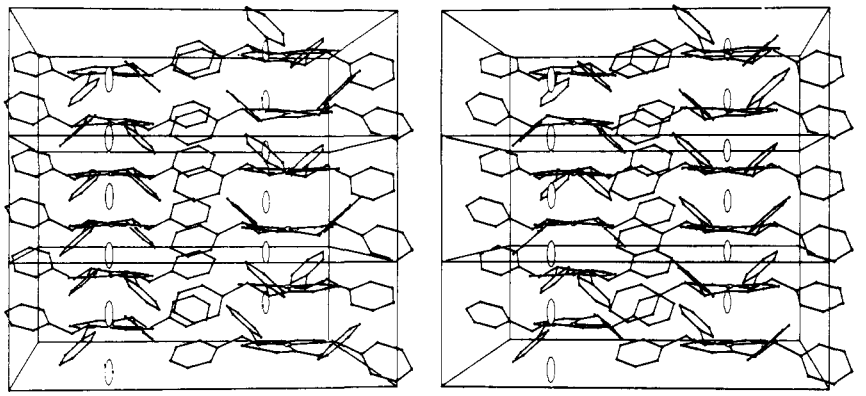

Figure 2. A stereoview of the unit cell of $Ni(dpg)_2I$. The *a* axis is horizontal to the right, the *b* axis is away from the reader, and the *c* axis is vertical from bottom to top. The vibrational ellipsoids of the Ni and I atoms are drawn at the 50% level. All other atoms are drawn arbitrarily small.

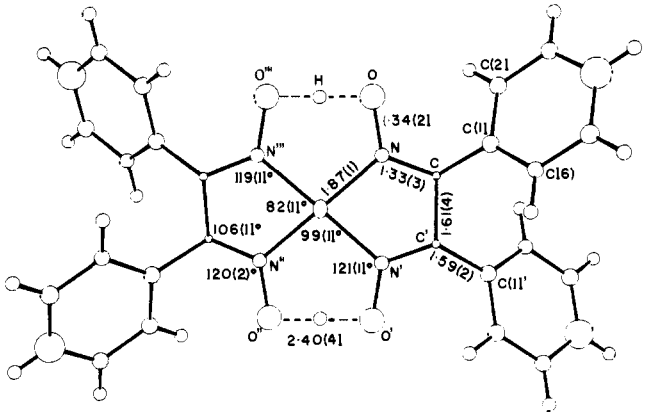

Figure 3. A drawing of the $Ni(dpg)_2^{0.20+}$ cation showing the numbering scheme used and some relevant bond lengths and angles. The vibrational ellipsoids are drawn at the 50% level, except hydrogen atoms, which are arbitrarily small.

Å).[7a,8c] In all cases where an iodinated and noniodinated material can be compared, the iodination has brought about a significant contraction in the Ni-Ni distance. Despite this contraction, the metal-metal distances in these stacked compounds are still appreciably larger than in face-to-face metallomacrocycle dimers such as $[Ni(C_{14}H_{18}N_4)]_2(CF_3SO_3)_2$,[35] which contains two eclipsed B units. Here spectral

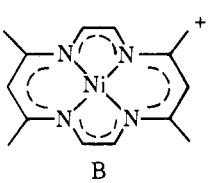

B

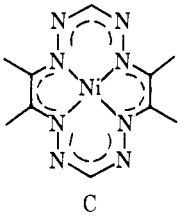

C

studies[35a] suggest a weak metal-metal interaction, and the Ni-Ni distance is found to be 3.063 (1) Å,[35b] Analogous examples include $[Ni(C_{10}H_{14}N_8)]_2$,[36] containing structural unit C, where there is considerably stronger metal-metal communication and where Ni-Ni = 2.788 (2) Å, and $[Ni(dmgBF_2)_2]_2$,[37] where Ni-Ni = 3.21 Å. As a point of reference, the distance in nickel metal, 2.49 Å,[38] is shorter still.

The $Ni(dpg)_2$ unit has crystallographically imposed point symmetry 222, so it is not crystallographically required to be planar. In fact, the molecule is rather puckered, This is shown clearly in Table VI by the deviations of the atoms from the least-squares planes. In plane 5, consisting of the four N atoms, each N atom is displaced alternately above and below the plane by 0.12 (2) Å. Similarly, within the chelate ring the two C atoms are displaced above and below the mean plane by 0.20 (3) Å. The large N-C-C′-N′ torsion angle of 33 (2)° about the C-C′ bond is a further indication of the nonplanarity of the chelate ring. This puckering of the inner core of the $Ni(dpg)_2$ unit appears to result from the close approach of the two adjacent phenyl groups on the chelate and also from the close approach of the molecules along the stacking axis. Table V shows that there are several short nonbonded contacts primarily involving the phenyl rings. The distortions of the C-C(1)-C(2) and C-C(1)-C(6) angles (see Table V) from their ideal values of 120° also seem to result from the above interactions. To minimize these interactions the adjacent phenyl rings are tipped 64.8° from each other and 36.8° from the chelate plane.

All bond lengths and angles in the $Ni(dpg)_2$ unit, at −160 °C, are essentially identical with those in the room temperature structure determination[7c] and agree well with those reported in other nickel tetraazamacrocycle complexes. The $Ni(dpg)_2I$ results are of limited accuracy owing to the predominance of iodine scattering and the presence of diffuse intensities. The

Table VI. Weighted Least-Squares Planes

plane no.	Plane Equation: $Ax + By + Cz - D = 0$, with x, y, z, in Crystal Coordinates A, Å	B, Å	C, Å	D, Å	
1	2.130	−2.130	−6.370	0.528	
2	2.130	−2.130	6.370	−2.657	
3	1.088	1.088	6.426	−1.607	
4	1.088	1.088	−6.426	1.607	
5	0.000	0.000	6.446	−1.612	
6	2.091	12.891	4.840	2.693	phenyl
7	12.891	2.091	−4.840	−0.287	phenyl′

	Deviations from the Planes (Å) ×10² plane no.				
atom	1	2	3	4	5
Ni					0
N	7 (2)			−1 (2)	12 (2)
O				1 (2)	
C	−20 (3)				
N′	−7 (2)		−1 (2)		−12 (2)
O′			1 (2)		
C′	20 (3)				
N″		−7 (2)	1 (2)		12 (2)
O″			−1 (2)		
C″		20 (3)			
N‴		7 (2)		1 (2)	−12 (2)
O‴				−1 (2)	
C‴		−20 (3)			

Dihedral Angles between Planes					
plane A	plane B	angle, deg	plane A	plane B	angle, deg
1	2	162.5	3	4	171.1
1	6	143.2	6	7	115.2

Ni–N distance of 1.868 (15) Å is normal, being close to the value of ca. 1.85 Å observed in several four-coordinate Ni(II) complexes.[39] This contact is significantly shorter than the Ni–N distances observed in the four-coordinate Ni(II) porphyrins (1.902 (5) to 1.98 (1) Å).[40-43] However, it is close to the average Ni–N distance of 1.874 (3) Å in $[Ni(C_{14}H_{18}N_4)]_2(CF_3SO_3)_2$[35b] and 1.832 (5) Å in $[Ni(C_{10}H_{14}N_8)]_2$.[36] The N–C distance of 1.33 (3) Å and the N–O distance of 1.34 (3) Å in the coordinated diphenylglyoximate ligand are comparable with the corresponding distances in $Ni(dmg)_2$,[11] i.e., 1.30 (3) and 1.35 (2) Å, respectively. The distances C–C′ (1.61 (4) Å) and O–O (2.40 (4) Å) in the present structure also compare favorably with the analogous $Ni(dmg)_2$ parameters of 1.54 (3) and 2.40 (2) Å, respectively.

As already noted in the discussion of the structure solution (Experimental Section) the iodine atoms in $Ni(dpg)_2I$ are disordered along the c axis in such a manner that the form of the iodine (I_2, I_3^-, I_5^-, I^-, or a mixture thereof [9]) cannot be determined from the Bragg scattering. Analysis of the diffuse scattering pattern enables us to reject models consisting of simple chains of I_2 or I_3^- units; the data are consistent with I_5^-[32] being the predominant species. Spectral data (vide infra) are also consistent with the presence of I_5^- units.

Resonance Raman Studies. In an effort to obtain additional information on the nature of the iodine-containing species in $Ni(dpg)_2I$ and $Pd(dpg)_2I$, solid state resonance Raman[45] vibrational spectroscopic studies were undertaken. As will be seen, this method can provide valuable structural information on polyiodide molecular structure and is immune to diffraction-related problems such as disorder and noncrystallinity. Each type of polyiodide molecule gives rise to a characteristic Raman scattering spectrum, and the resonant enhancement with typical visible laser excitation frequencies is generally sufficient so that iodine-centered vibrational transitions are not obscured by modes from other oscillators in the crystal. A complete description of our resonance Raman studies on a wide variety of polyiodide compounds will be presented elsewhere.[10c] In this discussion we summarize the theory and results pertinent to differentiating various species which could occur in the channels of low-dimensional materials such as $Ni(dpg)_2I$ and $Pd(dpg)_2I$.

The intensity of a Raman transition, $I(\nu_r)$, averaged over all molecular orientations, can be expressed in terms of the Raman scattering tensor, $R_{\rho\sigma}$, as shown in the equation

$$I(\nu_r) = \frac{2^7\pi^5}{3^2c^4}\nu_r^4 I(\nu_0)\sum_{\rho\sigma}|R_{\rho\sigma}|^2 \qquad (3)$$

Here $I(\nu_0)$ is the intensity of the laser exciting line (at ν_0), ν_r is the frequency of the Raman scattered radiation, and c is the speed of light. It is possible to express $R_{\rho\sigma}$ in such a way as to incorporate both Herzberg-Teller coupling and Born-Oppenheimer nonadiabatic coupling.[45,46] Thus, according to the equation

$$R_{\rho\sigma} = A + B \qquad (4)$$

the Raman scattering tensor is the sum of terms which describe scattering arising from Franck-Condon allowed transitions involving a single excited electronic state (A terms) and those which derive intensity through vibronic coupling between two or more excited electronic states (B terms). For a transition from vibrational level i to j in the ground electronic state (gi to gj), these terms can be expressed as in the equations

$$A = \frac{1}{h}\sum\left[\frac{(g^0|\mu_\rho|e^0)(e^0|\mu_\sigma|g^0)\langle gj|ev\rangle\langle ev|gi\rangle}{\nu_{ev,gi} - \nu_0 + i\Gamma_{ev}} + \frac{[\rho\leftrightarrow\sigma]}{\nu_{ev,gi} + \nu_0 + i\Gamma_{ev}}\right] \qquad (5)$$

$$B = \frac{-1}{h^2}\sum_{e,v}\sum_{s,u}{}'\left[\frac{(g^0|\mu_\rho|s^0)(s^0|(\partial H/\partial Q)_0|e^0)(e^0|\mu_\sigma|g^0)\langle gj|su\rangle\langle su|Q|ev\rangle\langle ev|gi\rangle}{(\nu_{su,gi} - \nu_0 + i\Gamma_{su})(\nu_{ev,gi} - \nu_0 + i\Gamma_{ev})} + \frac{[\rho\leftrightarrow\sigma]}{(\nu_{su,gj} + \nu_0 + i\Gamma_{su})(\nu_{ev,gj} + \nu_0 + i\Gamma_{ev})}\right] \qquad (6)$$

Here $|e^0)$ is the adiabatic electronic wave function of excited electronic state e, evaluated at the equilibrium nuclear coordinates of the ground electronic state, g, μ is the dipole transition operator, and $|ev\rangle$ is the wave function of vibrational level v of state e. The terms $\nu_{ev,gi}$ in the denominator are the frequency separations between vibronic levels, and the Γ_{ev} denote damping terms describing the radiative widths of the vibronic states, ev. The symbol s denotes excited electronic states other than e, the prime on the summation excludes terms where $s = e$, and $(\partial H/\partial Q)_0$ represents the vibronic coupling operator describing how the electronic Hamiltonian varies with displacement along normal mode Q. This operator is evaluated at the ground-state nuclear coordinates and transforms as normal mode Q. The second term in each equation refers to the nonresonant case. It is seen from eq 5 and 6 that for A terms only the totally symmetric normal modes of molecular vibration are expected to be resonance enhanced, while for B terms only those vibrational modes which vibronically couple states s and e are expected to be enhanced. Those normal modes which transform the molecule from the ground-state nuclear configuration to an appreciably displaced nuclear configuration in an excited electronic state should, all other factors being equal, experience the greatest resonance enhancement.

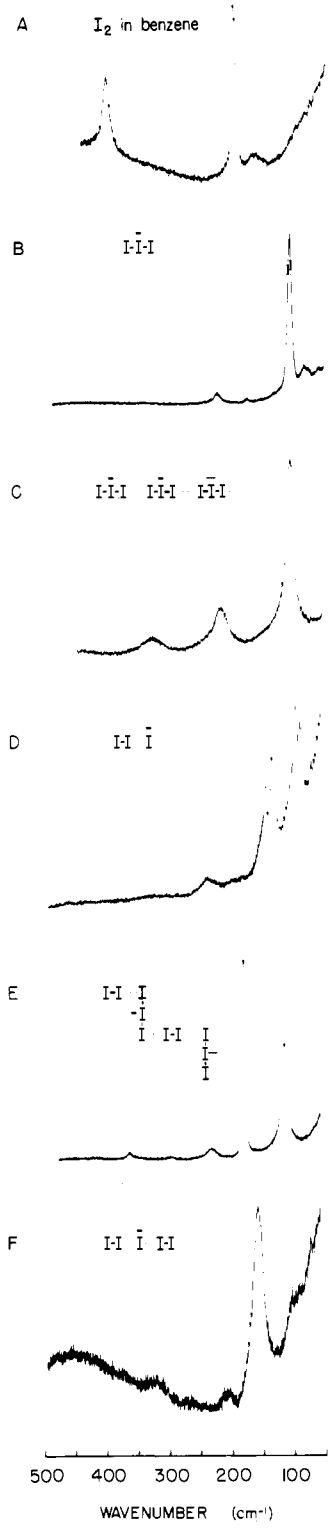

Figure 4. Resonance Raman spectra (5145 Å excitation) of (A) I_2 dissolved in benzene, (B) polycrystalline $(C_6H_5)_4As^+I_3^-$, (C) polycrystalline $(C_6H_5CONH_2)_2H^+I_3^-$, (D) polycrystalline $Cs^+I_3^-$, (E) polycrystalline $(phenacetin)_2H^+I_3^-\cdot I_2$, (F) polycrystalline $(trimesic\ acid\cdot H_2O)_{10}\cdot H^+I_5^-$.

In addition to the above relationships and the phenomena which follow from them, empirical information on force and interaction constants is required before polyiodide structural deductions can be made. Model compounds of known structure can provide such data. Figure 4A shows a solution resonance Raman spectrum of I_2; the intense stretching fundamental at 209 cm^{-1} is observed along with the characteristic[47] overtone progression. Figure 4B presents the spectrum of $(C_6H_5)_4^+I_3^-$,[48] which contains isolated, symmetrical (equal I-I distances) I_3^- units.[48] As is observed in all polyiodide resonance Raman spectra recorded to date,[10c] only the totally symmetric I-I stretching vibrations (for I_3^-, the in-phase stretching of the two oscillators) are appreciably enhanced with ν_0 = 4880-6471 Å excitation. The actual I-I stretching frequency in I_3^- is the average of the symmetrically (118 cm^{-1}) and antisymmetrically (145 cm^{-1}) coupled normal modes,[9,49] 132 cm^{-1}, which represents an appreciable lowering of the force constant from that in I_2. This feature illustrates an important point in understanding polyiodide electronic structure and vibrational spectra: molecular I_2 acts as a Lewis acid and coordination to Lewis base, e.g., I^-, weakens the I-I bonding. Thus the I-I distance in I_2 is 2.72 Å while in I_3^- it is near 2.92 Å.[9] Molecular orbital calculations on I_3^- also show that the highest occupied molecular orbital has I-I antibonding character.[50] When I_3^- units are placed in a linear chain $[((C_6H_5)CONH_2)_2H^+I_3^-]$[51] the electronic spectral visible maximum shifts somewhat,[10c,51] and I_3^- scattering is again observed (Figure 4C) but with a more pronounced overtone progression. The partially oxidized complexes $Ni(bqd)_2I_{0.5}$[7b,10a] and Ni(Pc)I[8a-c] are examples of quasi-one-dimensional stacked electrically conductive metallomacrocyclic systems with chains of I_3^- parallel to the stacking direction.[52] Examples are also known where crystal forces produce distortion of the I_3^- ions.[53] In CsI_3, I-I distances of 2.83 (2) and 3.03 (2) Å are observed,[48] and two resonance-enhanced I-I stretching modes at 146 and 99 cm^{-1} (further split by small solid-state effects[10c,53]) are evident in the Raman spectrum (Figure 4D). Two other kinds of polyiodide structural motifs are also known. Crystallographically identifiable combinations of I_2 and I_3^- are observed in a number of materials such as $(Cs^+)_2(I_3^-)_2\cdot I_2$,[55a] $(phenacetin)_2H^+I_3^-\cdot I_2$,[55b] and $(C_2H_5)_4N^+I_3^-\cdot 2I_2$.[55c] The presence of *both* I_2 and I_3^- units is clearly evident,[10c] as exemplified by the spectrum of the phenacetin compound (Figure 4E). The I-I distance in the "I_2"[54] unit has lengthened to 2.748 (2) Å, which is reflected in the lower "I_2" ν_{I-I} frequency of 185 cm^{-1}; the "I_3^-" totally symmetric stretch occurs at 119 cm^{-1}. The dotted lines in the structural drawing of Figure 4E represent relatively long I-I distances of 3.550 (2) Å, A very weak emission at 160 cm^{-1} may evidence slight distortion of the I_3^- moiety. The bands at frequencies above 200 cm^{-1} can be assigned to overtone and combination bands of the above modes; this assures that the I_3^- and I_2 oscillators are in close proximity and that the observed scattering pattern does not arise from a mixture of different compounds. Completely analogous spectra are observed for the other two $I_2 + I_3^-$ model compounds discussed above,[10c] with the only difference being that the distorted (I-I = 2.84 and 3.00 Å) I_3^- units in Cs_2I_8[55a] give rise to a strong band at 150 cm^{-1} in addition to one at 105 cm^{-1}. This is completely analogous to the above-mentioned situation in CsI_3. Examples have also been reported where I^- is symmetrically bound to two I_2 units. This species can be considered as the I_5^- ion and both linear $[(trimesic\ acid\cdot H_2O)_{10}\cdot H^+I_5^-]$[32] and bent $[(CH_3)_4N^+I_5^-]$[56] cases have been identified. The resonance Raman spectrum of the trimesic acid compound, which has chains of linear I_5^-, is illustrated in Figure 4F. The "I_2"[54] I-I stretching frequency of 160 cm^{-1} suggests that the I^- must now distribute electron density between two Lewis acid I_2 units and that the attendant lowering of the I-I force constant is not as great as in I_3^-. The reported $^{32}I_2$ I-I distance of 2.74 Å is in accord with this. The weak scattering at 107 cm^{-1} may be due to symmetric stretching which is predominantly $I_2 \leftarrow \bar{I} \rightarrow I_2$ in character;[57] the I-I distance is 3.24 Å.[32] The selection rules for $D_{\infty h}$ I_5^- also predict a Raman-active π_g bending mode, which may occur at even lower frequency. The spacing between I_5^- units in this structure is 3.50 Å. In summary, results for the various model

Table VII. Raman Scattering Data[a,b]

$Ni(dpg)_2$: 418 (ms), 113 (w, br), 91 (vvw), 71 (vw)
$Ni(dpg)_2I$: 447 (w), 407 (vw), 325 (mw, br), 270 (w, br), 210 (vw, br), 162 (vs), 107 (w)
$Pd(dpg)_2$: 405 (vw), 166 (vw), 133 (vw), 82 (w, sh), 69 (vw)
$Pd(dpg)_2I$: 467 (vvw), 446 (vw), 427 (vvw), 323 (mw), 266 (w, br), 210 (vw, br), 160 (vs), 104 (mw)
(trimesic acid·H_2O)$_{10}$·HI_5: 206 (w, br), 162 (vs), 104 (w, br), 75 (vw)

[a] Polycrystalline samples, 5145 Å excitation. [b] In cm^{-1}; s = strong, m = medium, w = weak, v = very, br = broad, sh = shoulder.

compounds discussed form the basis for the Raman characterization of polyiodide structure in the $M(dpg)_2I$ series. The polyiodide spectra observed are generally rather insensitive in pattern to the laser exciting frequency (ν_0 = 4880-6471 Å),[10b,c] and this is in agreement with the substantial breadth of most polyiodide solid state electronic spectra.[10c,51] This situation will be illustrated in a later section (vide infra). In most cases the polyiodide electronic spectra consist of a number of severely overlapped transitions which have not been assigned with certainty.[58] The electronic transitions associated with large resonance Raman enhancement no doubt involve a significant structural change in going to the excited electronic state.[45]

Resonance Raman spectra of solid $Ni(dpg)_2$, $Ni(dpg)_2I$, $Pd(dpg)_2$, and $Pd(dpg)_2I$ are shown in Figure 5 and numerical data are presented in Table VII; spectra recorded at 8 °K are identical. Discussion of the optical spectra is deferred to the following section. Both iodides feature strong Raman scattering at 161 cm^{-1} and a weaker transition at ca. 107 cm^{-1}; overtone and combinations of these emissions are observed at ca. 210 w (2 × 107), 268 mw (161 + 107), and 324 mw (2 × 161) cm^{-1}. That these transitions are assignable to a polyiodide and not to $M(dpg)_2$ units is supported by the observation that the analogous (and isostructural[14d]) $M(dpg)_2Br$ materials exhibit resonance-enhanced scattering at energies assignable to polybromide species, but only weak scattering in the $M(dpg)_2I$ region (156 cm^{-1}). Thus, the resonance-enhanced transitons at 161 and 107 cm^{-1} clearly arise from the polyiodide constituent. From the foregoing discussion two assignments seem most reasonable: a highly distorted I_3^- or an I_5^- moiety. As can be seen below, the same chromophore is present

$$I-I\cdots I^- \qquad I-I\cdots\bar{I}\cdots I-I$$

in each structure. Although a highly distorted I_3^- was at first considered a distinct possibility,[7c,d] that such an extreme distortion should take place in the nonpolar channels of the $M(dpg)_2$ crystal structure is not clear and not physically realistic.[53] Furthermore, such a degree of distortion is not evident in the Raman spectra of any model compound examined to date.[10c] On the other hand, the correspondence between the $M(dpg)_2I$ Raman spectra and those of the I_5^- chain model compound (trimesic acid·H_2O)$_{10}$·$H^+I_5^-$ (Figure 4) is strikingly close and argues persuasively for I_5^- as the predominant species. The band at 107 cm^{-1} in the $M(dpg)_2I$ spectra is, by analogy to the trimesic acid pentaiodide results, also attributable to I_5^-. There is no evidence for free I_2 in the Raman spectra. In addition to these results, it will also be seen that the fully refined ^{129}I Mössbauer spectra and the optical spectra are in good agreement with the I_5^- formulation. Efforts to obtain with far-infrared techniques further vibrational spectroscopic information on the $M(dpg)_2I$ polyiodide component were unsuccessful. Comparison of spectra for the $M(dpg)_2$, $M(dpg)_2I$, and $M(dpg)_2Br$ compounds (see Experimental Section for data) revealed no significant absorption which could be assigned to an infrared-active I-I stretching transition;[9,49] these bands are apparently obscured by intense $M(dpg)_2$-centered normal modes.

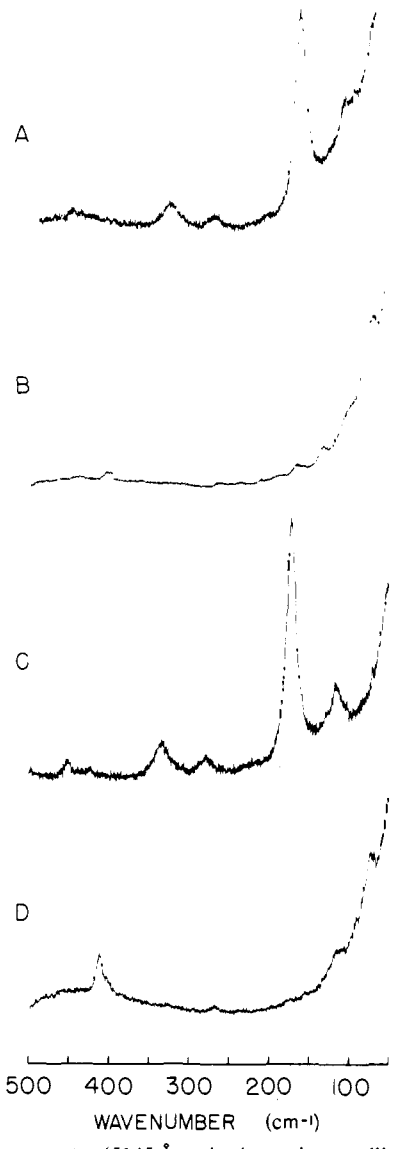

Figure 5. Raman spectra (5145 Å excitation, polycrystalline samples) of (A) $Pd(dpg)_2I$, (B) $Pd(dpg)_2$, (C) $Ni(dpg)_2I$, (D) $Ni(dpg)_2$.

The Raman spectra of both $M(dpg)_2$ and $M(dpg)_2I$ materials reveal weak bands at energies above 400 cm^{-1} (see Table VII for data), which are too narrow to be polyiodide overtone or combination bands. Furthermore, the band positions are sensitive to the nature of M. We assign these emissions to vibrations within the $M(dpg)_2$ and $M(dpg)_2^{0.2+}$ units. Interestingly, in accord with the crystallographic data, there is no evidence for discrete $M(dpg)_2$ units in the $M(dpg)_2I$ materials (i.e., trapped valency). When the iodinated species are heated, iodine loss is accompanied by diminution of the $M(dpg)_2^{0.2+}$ "markers" and growth of the $M(dpg)_2$ "markers"; no spectra of intermediate species are observed. The internal coordinate changes associated with these bands are presumably analogous to the resonance-enhanced metal-ligand or metal-influenced ligand vibrations observed for porphyrins[45,60] and other metallomacrocycles.[46b,61]

Iodine-129 Mössbauer Studies. Recoilless 27.7-keV nuclear resonant absorption spectroscopy between the I_{ground} = 7/2 and $I_{excited}$ = 5/2 nuclear levels of iodine-129 is an established physical method for investigating structure and bonding in iodine-containing materials.[62] For characterizing polyiodides, it is a useful supplement to resonance Raman spectroscopy

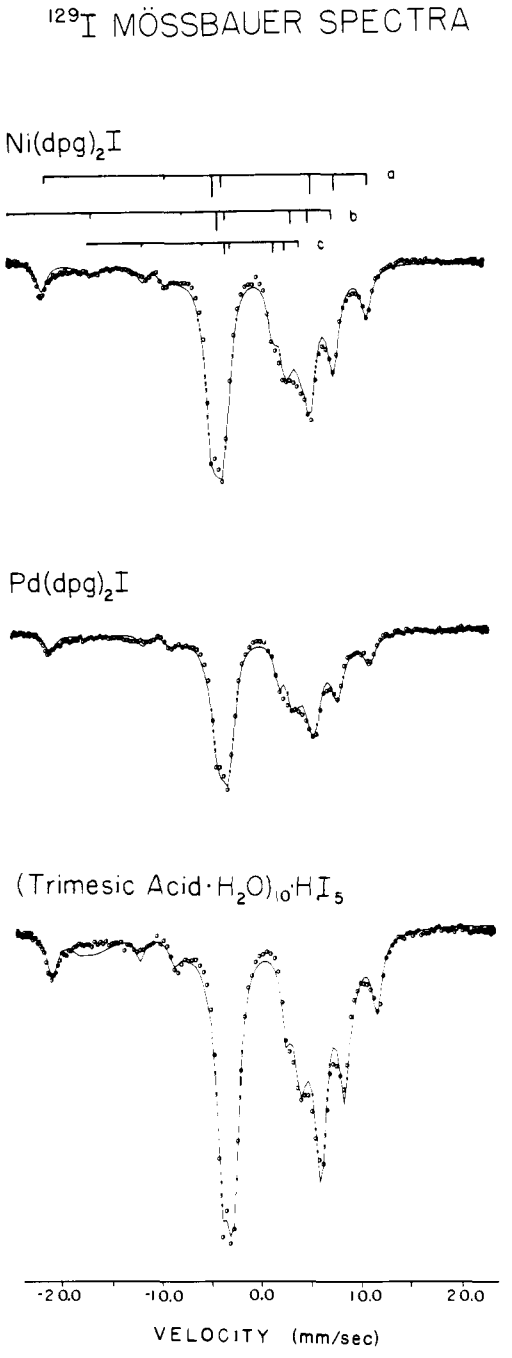

Figure 6. Iodine-129 Mössbauer spectra of the indicated compounds as solids at 4 K. The solid lines represent the best computer fit to the data points. Stick figures representing contributing transitions are shown for the Ni(dpg)$_2$I spectrum. Isomer shifts are referenced to ZnTe.

since it can readily identify I^- (a spherically symmetrical electric field gradient about the iodine nucleus gives rise to zero quadrupole splitting).[7,10] In addition, iodine-129 Mössbauer spectroscopy can be used for quantitative evaluation of relative site populations.[10,62] The observed spectrum will be a superposition of the quadrupole patterns of the dissimilar iodine atoms in proportion to the respective populations. This ability to evaluate site populations is important in cases where resonance Raman techniques have not been sufficiently calibrated for quantitative assessments or where it is believed that unusual or previously unknown kinds of polyiodides are present. The distorted I_3^- vs. I_5^- question discussed above was part of the motivation for the present study.

Samples of Ni(dpg)$_2$^{129}I and Pd(dpg)$_2$^{129}I were prepared as described in the Experimental Section. Mössbauer spectra obtained at 4 K, are shown in Figure 6, along with computer-generated theoretical spectra for the best fit to the data (see Experimental Section for details of this procedure). It will be seen that the data are in best agreement with an essentially $D_{\infty h}$ I_5^- species. For comparison, we also present the spectrum[10b] of the I_5^- chain compound (trimesic acid·H$_2$O)$_{10}$·H$^+$ $^{129}I_5^-$.[32] Stick spectra showing the quadrupole patterns for the three inequivalent iodine sites in Ni(dpg)$_2$I are presented in the same figure. Numerical values of the parameters obtained from the spectral fitting procedure with their estimated standard deviations are given in Table VIII. The isomer shift and quadrupole coupling constants for corresponding sites in the three compounds are, within experimental error, very similar. Values of these parameters[63] are compared with those for symmetrical[64a,b] and distorted[64b,c] I_3^- in Chart I.

Table VIII. Iodine-129 Mössbauer Parameters

	Ni(dpg)$_2$I	Pd(dpg)$_2$I	(trimesic acid·H$_2$O)$_{10}$H$^+$I$_5^-$
	Site 1		
δ, mm/s[a]	1.20 (3)	1.19 (3)	1.15 (3)
e^2qQ, MHz[b]	−1778 (5)	−1749 (5)	−1777 (5)
Γ, mm/s[c]	1.24 (5)	1.36 (7)	1.15 (5)
rel population	2.12 (10)	1.96 (10)	1.96 (10)
	Site 2		
δ, mm/s	0.47 (5)	0.57 (5)	0.53 (5)
e^2qQ, MHz	−1308 (8)	−1354 (8)	−1404 (8)
Γ, mm/s	1.68 (5)	1.34 (5)	1.75 (5)
rel population	2.22 (10)	1.78 (10)	1.97 (10)
κ[d]	0.257 (5)	0.209 (9)	0.138 (5)
	Site 3		
δ, mm/s	0.161 (8)	0.201 (10)	0.13 (5)
e^2qQ, MHz	−861 (5)	−898 (6)	−965 (5)
Γ, mm/s	1.06 (4)	1.01 (4)	1.04 (4)
rel population	1.00	1.00	1.00
Misfit, %[d]	0.65 (3)	0.64 (3)	0.70 (4)
χ^2	2856	2112	1400

[a] Vs. ZnTe. [b] For ^{129}I. [c] Line width. [d] Defined in Experimental Section.

Chart I

δ, mm/s	0.25	1.48	0.25	0.11	1.14	−0.24
$e^2q^{129}Q$, MHz	−808	−1725	−808	−1036	−1787	−618
rel site population	1.00	1.23	1.00			
	{RuCp$_2$^{129}I}^{129}I$_3$[64a,b]			Cs^{129}I$_3$[64b,c]		
δ, mm/s	0.52	1.20	0.18	1.20	0.52	
$e^2q^{129}Q$, MHz	−1331	−1764	−880	−1764	−1331	
rel site population	1.00	1.02	1.00	1.02	1.00	
		M(dpg)$_2$^{129}I[63]				

The above assignment of δ and e^2qQ to particular sites in I_5^- is that most consistent with bonding arguments (vide infra). It is also apparent from the values of the refined Mössbauer parameters in Table VII that iodine site populations in the M(dpg)$_2$I materials are known with good but not as great a precision as δ and e^2qQ. For this reason a number of experiments were conducted to determine to what degree the populations given in Table VIII were the most accurate representation of the proportions of possible sites present and what choices of polyiodides could be clearly rejected. In an attempt to fit the data to two inequivalent iodine sites, relative populations were constrained to 1:1 and to 1:2 (symmetrical I_3^-). This resulted in a marked deterioration of the goodness of fit parameter "Misfit" (see Experimental Section) from the values shown in Table VIII. This was true regardless of the choice of δ, e^2qQ, and line width. Similarly, fitting the data to three

inequivalent iodine sites with relative site population 1:1:1 (unsymmetrical I_3^-) resulted in very poor agreement between experimental and calculated spectra for a wide range of reasonable δ, e^2qQ, and line width values. On the other hand, constraining the relative populations for three inequivalent iodine sites to 2:2:1 (e.g., symmetrical I_5^-) produced little change in the value of "Misfit" when compared with a three-site fit with no constraints on the relative populations. Thus, we conclude from the ^{129}I Mössbauer spectroscopy, as we concluded from resonance Raman spectroscopy, that the predominant iodine-containing species in $Ni(dpg)_2I$ and $Pd(dpg)_2I$ is I_5^-.

On the basis of the present study, no extraneous iodine-containing species could be detected in the crystalline $M(dpg)_2{}^{129}I$ materials. It is, however, worth considering to what level of contamination other iodine-containing species might be present, but remain undetected, by ^{129}I Mössbauer spectroscopy. Based on known parameters[62] for I^- ($\delta = -0.51$ mm/s, $e^2q^{129}Q = 0.00$ MHz) and for I_2 in frozen hexane solution ($\delta = +0.98$ mm/s, $e^2q^{129}Q = -1586$ MHz), we estimate that these species can be present to no greater than 5 and 3 mol %, respectively. The possibility that small amounts of either symmetrical or distorted I_3^- are present was also considered. It can be seen from published isomer shift and quadrupole coupling constants for triiodides[62,64] that many of the observed transitions will overlap with the I_5^- transitions, so that the maximum level of I_3^- impurities present can only be estimated from the relative site populations. Although we have found no direct evidence for any significant amount of I_3^-, symmetrical or distorted, we estimate that less than 5 molecule % I_3^- impurity would be undetectable.

Examination of the isomer shift and quadrupole coupling constants for the I_5^- species yields information on charge distribution and bonding which can be meaningfully compared with results obtained for symmetrical and unsymmetrical I_3^-. Using a Townes-Dailey approach[65] as summarized by Ruby and Shenoy,[65c] the iodine-129 isomer shift vs. ZnTe can be expressed as a function of the number of 5s electron holes, h_s, and the number of 5p electron holes, h_p:

$$\delta = -9.2h_s + 1.50h_p - 0.54 \text{ (mm/s)} \quad (7)$$

Alternatively, the effective 5p electron imbalance, U_p, can be calculated directly

$$U_p = -e^2q_{mol}{}^{129}Q/e^2q_{atom}{}^{129}Q \quad (8)$$

from the ratio of the experimental value of the nuclear quadrupole coupling constant in the molecule under examination ($e^2q_{mol}{}^{129}Q$) to that of atomic iodine ($e^2q_{atom}{}^{129}Q = 1670$ MHz, $U_p = 1$). Here U_p is defined in eq 9 in terms of the 5p electron populations in the three Cartesian spatial directions.

$$U_p = -U_z + \tfrac{1}{2}(U_x + U_y) \quad (9)$$

For axial symmetry, the asymmetry parameter is zero and $U_x = U_y$.[62,66] Prior studies[62,64] have shown that in polyiodides such as I_2 and I_3^- the bonding largely if not exclusively involves the p_z orbitals;[62,64a] hence, it can be assumed that $h_s \approx 0$ and $U_x = U_y \approx 2$. From eq 7-9 it can be seen that U_p, U_z, and thus the approximate charges on the iodine atoms can be calculated from two independent approaches.[66] The agreement of these two methods serves as an additional check on the quality of the data and the internal consistency of the parameter values obtained.[66c] Chart II sets out the calculated charge distributions (eq 7 and 8) for symmetrical I_3^-, distorted I_3^-, and I_5^-.[67] The charge distribution results based upon quadrupole splitting data are probably slightly more reliable in most cases since the probable error in a large e^2qQ value typically represents a smaller percentage of the derived charge distribution. In terms

Chart II

from δ	−0.47	+0.35 (+0.25)[68]	−0.47	−0.56	+0.13	−0.72
from e^2qQ	−0.49	+0.07	−0.49	−0.35	+0.11	−0.60

from δ	−0.29	+0.17	−0.42	+0.17	−0.29
from e^2qQ	−0.20	+0.10	−0.44	+0.10	−0.20

of electronic structure, the results of the above calculations reveal that distorting the I_3^- ion is equivalent, in a first-order approximation, to pulling an I^- away from I_2. That is, the resulting values of isomer shifts and quadrupole coupling constants tend toward I_2 and I^- in that the charges on the "departing" iodide become more negative while the charges on the iodine atoms in the emerging I_2 unit tend toward neutrality. The I_5^- molecule exhibits a similar pattern in the "I_2" fragments, i.e., the charge distribution is more nearly equal and the charge concentration less negative than in I_3^-. Interestingly, the central iodine atom in I_5^- does not possess as great a negative charge as the "departing" iodine atom in distorted I_3^-. This can be rationalized by the observation mentioned in the Raman discussion, that the "I^-" in I_5^- must share its electron density with two I_2 Lewis acid units. Reversing the assignment of the two highly populated sites in I_5^- results in an ion with positive charge on the two outer iodine atoms and negative charge on the three inner iodine atoms. In terms of chemical bonding[50] and the foregoing discussion, this must be regarded as highly unlikely.

Electronic Spectra. Electronic absorption spectra of the $M(dpg)_2$ and $M(dpg)_2I$ materials, M = Ni and Pd, as Nujol mulls are presented in Figures 7A-D. These data as well as those for chloroform solutions are compiled in Table IX. The spectral features of $Pd(dpg)_2$ and $Ni(dpg)_2$ are closely analogous to those of other stacked d^8 palladium and nickel bisglyoximates.[69] There is also a close similarity in transition energies. Furthermore, the two lowest energy spectral transitions in the polycrystalline $M(dpg)_2$ samples are not observed in solution, again a distinctive characteristic of stacked bisglyoximate systems. Thus, the 515-nm absorption in $Ni(dpg)_2$ and the 445-nm absorption in $Pd(dpg)_2$ can be correlated with stacked glyoximate transitions[69] which are found to be polarized parallel to the chain direction in single-crystal studies[69] and which ligand[70] and metal[70b,71] substitution as well as pressure dependence[69b,72] reveal to be highly sensitive to the intrastack metal-metal separation. These spectral features have been assigned to intramolecular $nd_{z^2} \rightarrow (n+1)p_z$ transitions which borrow intensity from intermolecular metal $\rightarrow$ metal charge transfer transitions.[69] In addition, the $(n+1)p_z$ orbitals may be mixed with ligand π^* molecular orbitals.[69a] The next highest energy bands (435 nm for $Ni(dpg)_2$ and 365 nm for $Pd(dpg)_2$) are analogous to those assigned to metal to ligand ($d\pi \rightarrow \pi^*$) charge transfer absorptions.[69] The energies of such transitions are generally rather insensitive to metal-metal separation.[69] Upon halogenation of the $M(dpg)_2$ materials, several noteworthy changes occur in the spectra (Figures 7A and 7C). A very broad transition, centered at ca. 675 nm, appears. Though such a transition might, a priori, be associated with mixed valency,[6b,73] comparison with the spectrum of the model I_5^- chain compound, (trimesic acid·$H_2O)_{10}$·$H^+I_5^-$, provides a persuasive argument for assignment as being largely a polyiodide transition. Indeed, polyiodide electronic spectra are quite distinctive and can sometimes be employed for qualitative structural assignments.[10c,74] Thus, broad absorptions centered near 700 nm are found in I_5^- chain compounds. The other spectral feature which is evident upon $M(dpg)_2$ halogenation is the disappearance or weakening of the long-wavelength $nd_{z^2} \rightarrow (n+1)p_z$ transitions and the appearance of a new band at 566 nm in $Ni(dpg)_2I$ and at 505 nm in $Pd(dpg)_2I$. In the absence of polarized single crystal

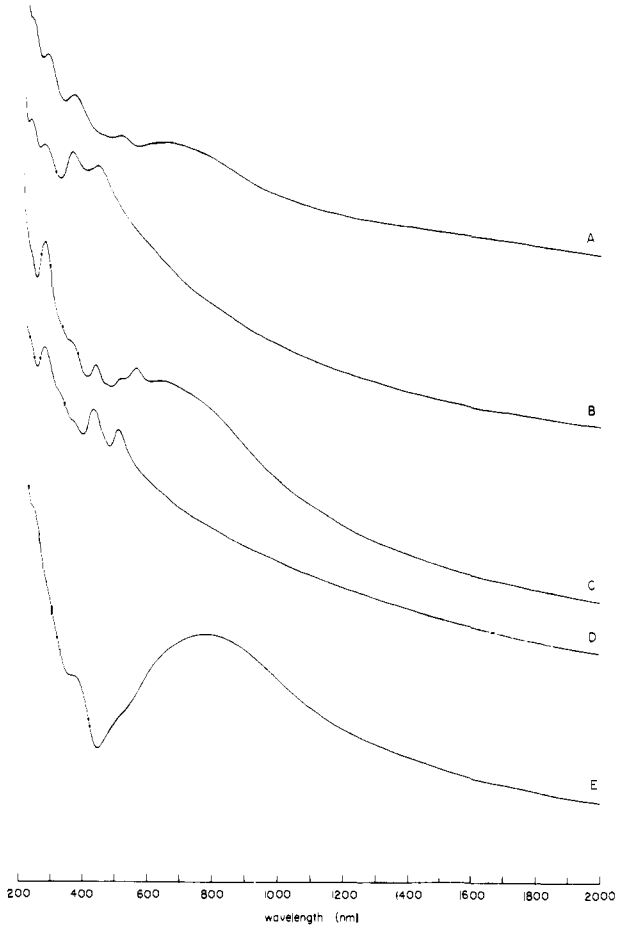

Figure 7. Electronic spectra (polycrystalline samples as Nujol mulls) of (A) $Pd(dpg)_2I$, (B) $Pd(dpg)_2$, (C) $Ni(dpg)_2I$, (D) $Ni(dpg)_2$, (E) (trimesic acid·H_2O)$_{10}H^+I_5^-$.

Table IX. Electronic Spectral Data in nm ($\times 10^3$ cm^{-1})[a,b]

compd	Nujol mull	$CHCl_3$ solution
$Ni(dpg)_2$	285 (35.1)	273 (36.6)
	335sh (29.9)	357 (28.0)
	372sh (26.9)	405 (24.7)
	435 (23.0)	460sh (21.7)
	515 (19.4)	
$Ni(dpg)_2I$	286 (34.9)	
	370sh (27.0)	
	443 (22.6)	
	520 (19.2)	
	566 (17.7)	
	675br (15.4)	
$Pd(dpg)_2$	235 (42.6)	243 (41.1)
	278 (36.0)	266 (37.6)
	365 (27.4)	324 (30.9)
	445 (22.5)	410sh (24.4)
$Pd(dpg)_2I$	235 (42.6)	
	278 (36.0)	
	362 (27.6)	
	456sh (21.9)	
	505br (19.8)	
	675 (15.4)	

[a] sh = shoulder, br = broad. [b] Data in parentheses given in cm^{-1}.

data[75] all that can be remarked about the origin of these transitions is that the data are consistent with an expected red shift of the aforementioned $nd_{z^2} \rightarrow (n+1)p_z$ transitions on contraction of the metal-metal separation. The energy shifts for the nickel and palladium absorptions are comparable, i.e., 9 and 12%, respectively, as are the contractions in metal-metal distances, i.e., 3.55 → 3.27 and 3.52 → 3.26 Å, respectively.

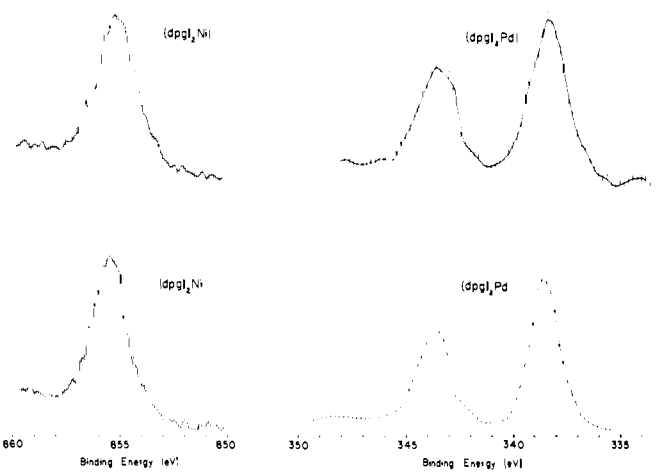

Figure 8. X-ray photoelectron spectra of the indicated compounds in $2p_{3/2}$ (Ni) and $3d_{5/2}$, $3d_{3/2}$ (Pd) regions. Traces are the result of 100–200 computer-averaged scans.

Table X. X-ray Photoelectron Spectroscopic Data for Metal Diphenylglyoximates

material	ionization	binding energy, eV	fwhm,[a] eV
$Ni(dpg)_2$	Ni $2p_{3/2}$	855.5 (5)	1.88
$Ni(dpg)_2I$	Ni $2p_{3/2}$	855.3 (5)	1.86
$Pd(dpg)_2$	Pd $3d_{3/2}$,$3d_{5/2}$	343.8 (4), 338.6 (4)	1.88, 1.87
$Pd(dpg)_2I$	Pd $3d_{3/2}$, $3d_{5/2}$	343.8 (4), 338.8 (4)	1.84, 1.85

[a] Full peak width at half maximum.

X-ray Photoelectron Spectra. XPS[76] data can provide useful information on the electronic structure of mixed-valence materials[77] when they are acquired[78] and interpreted with care.[79] In the present case, such data offered the possibility of assessing to what degree the fractional oxidation states in $Ni(dpg)_2I$ and $Pd(dpg)_2I$ might be localized, i.e., to what degree discrete sites such as Ni^{2+} and Ni^{3+} or Ni^{4+} might be present (type I or type II mixed valency).[73] The rapid XPS time scale (ca. 10^{-18} s) is particularly advantageous for this purpose.[76] In the case of a type III system, XPS offered the possibility of detecting major changes in charge distribution accompanying partial oxidation. Since XPS is a surface technique, the presence of iodine was continuously monitored during the $M(dpg)_2I$ studies to ensure that the uniodinated species were not being produced by the high vacuum or X-ray bombardment. In Figure 8 are presented $2p_{3/2}$ spectra of $Ni(dpg)_2$ and $Ni(dpg)_2I$ and $3d_{5/2}$, $3d_{3/2}$ spectra of $Pd(dpg)_2$ and $Pd(dpg)_2I$; data are set out in Table X. The important observations to be made are that the binding energies and line widths of corresponding $M(dpg)_2$ and $M(dpg)_2I$ materials, while in good agreement with literature data for nickel[76,80] and palladium[76,81] complexes, do not differ significantly from each other. There is no evidence of trapped valence or of appreciable change in metal atom charge in the halogenated materials. The absence of detectable "shake-up" satellites (core ionization plus molecular electronic excitation) in the nickel spectra is in agreement with the diamagnetism and square-planar coordination geometry.[80] Attempts to clean the surface of the iodinated materials by argon ion etching resulted in halogen loss. Element loss resulting from argon ion bombardment has been observed before.[82,83]

Electrical Conductivity. Single-crystal measurements of the

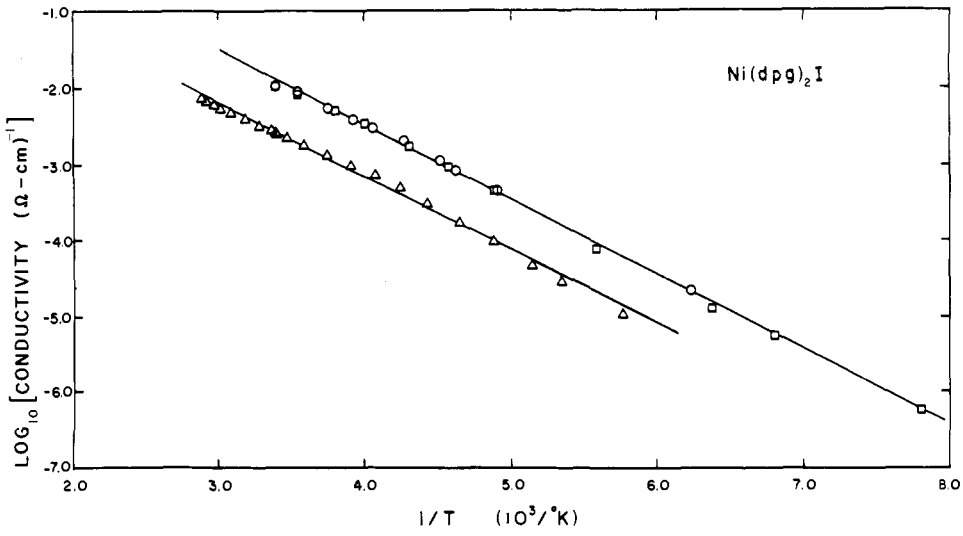

Figure 9. Electrical conductivity (dc) in the crystallographic *c* direction of representative $Ni(dpg)_2I$ crystals as a function of temperature.

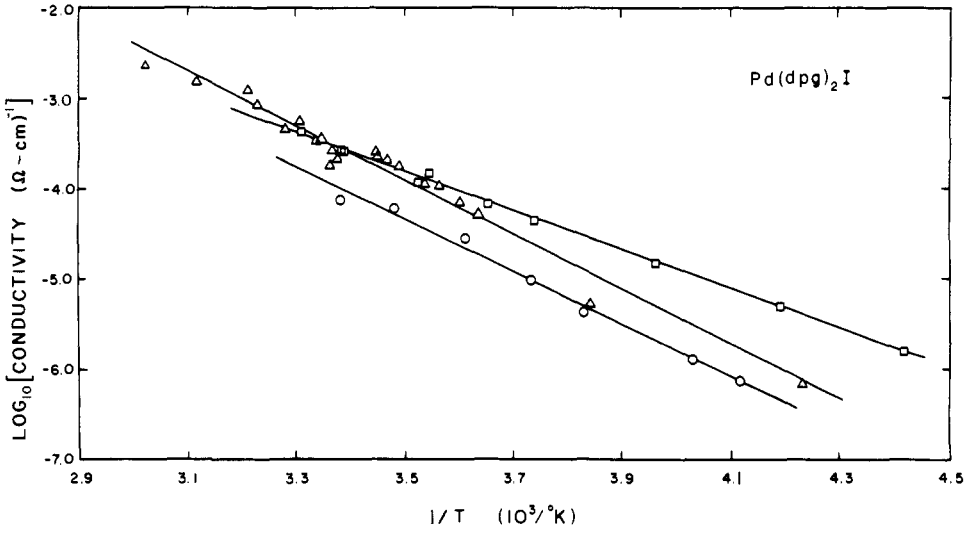

Figure 10. Electrical conductivity (dc) in the crystallographic *c* direction of representative $Pd(dpg)_2I$ crystals as a function of temperature.

electrical conductivities of the $M(dpg)_2$ and $M(dpg)_2I$ compounds were performed as a function of temperature by the standard four-probe technique (see Experimental Section for details). The needle-like morphology of the crystals precluded measurements in any direction other than parallel to the molecular stacking direction.

In Figures 9 and 10 are shown plots of representative conductivity data for $Ni(dpg)_2I$ and $Pd(dpg)_2I$. These as well as related data are summarized in Table XI. The range of conductivity is given at 300 K for all samples examined and is compared with the values for the corresponding unoxidized materials. In the case of the unoxidized samples, the values presented are an upper limit imposed by the sensitivity of the instrumentation and the geometry of the available samples; the actual conductivities may be one or more orders of magnitude less than 10^{-9} $(\Omega\ cm)^{-1}$. Also compared in Table XI are the dc and low-frequency ac conductivities measured on the same $M(dpg)_2I$ specimens. The excellent agreement obtained indicates a minimum of undesirable electrode-contact effects in the conductivity measurements.

As can be readily recognized from Figures 9 and 10, the data adhere closely to a linear dependence of ln σ vs. $1/T$ for the temperature range investigated. This behavior suggests that

Table XI. Single Crystal (*c* Axis) Electrical Conductivity Data for Metal Diphenylglyoximates

material	dc conductivity at 300 K, $(\Omega\ cm)^{-1}$ [a]	conductivity comparison at 300 K. $(\Omega\ cm)^{-1}$ [b] dc	ac (100 Hz)	Δ, eV[c]
$Ni(dpg)_2$	$<8 \times 10^{-9}$			
$Ni(dpg)_2I$	$2.3\text{-}11 \times 10^{-3}$	2.7×10^{-3}	3.0×10^{-3}	0.19 ± 0.1
$Pd(dpg)_2$	$<8 \times 10^{-9}$			
$Pd(dpg)_2I$	$7.7\text{-}47 \times 10^{-5}$	4.7×10^{-4}	5.0×10^{-4}	0.54 ± 0.11

[a] Range given for specimens examined. [b] Data for the same crystal. [c] From least-squares fit to eq 10.

the thermal activation model of the equation

$$\sigma = \sigma_0 e^{-\Delta/kT} \tag{10}$$

where there is a single activation energy, Δ, is the most appropriate description. In Table XI the average activation energy is presented for each material as obtained from a least-squares fit of the data to eq 10. The extent of variation for the values presented represents the largest deviation from the average for all samples shown. Especially for $Ni(dpg)_2I$, all

samples are remarkably similar in the slope of the ln σ vs. $1/T$ plot.

The data presented in Figures 9 and 10 were found to be reproducible when taken in order of either increasing or decreasing temperature. Although a slight fall-off in the slope of the ln σ vs. $1/T$ plots may occur at the highest temperatures shown,[84] attempts to reach higher temperatures were thwarted by sample decomposition. In these cases, returning the sample to room temperature did not restore the conductivity to its original value.

Two important features are obvious upon viewing the conductivity data. First, the iodination has brought about a very large increase in the facility of charge transport (ca. 10^7-10^8). Although a similar effect has been noted for other metallomacrocycle systems upon halogenation,[7a,b,8a,d] the bisdiphenylglyoximates represent the first case where the only feature of the donor crystal structure variable to change upon halogenation is the interplanar spacing. The second feature of note in the $M(dpg)_2I$ data is the dependence of the conductivity on the identity of M. The dependence is small, with $Ni(dpg)_2I$ being slightly more conductive. This result is surprising in view of the fact that the metal-metal distances are essentially equal on proceeding from nickel to palladium and the metal ionic radius increases by ca. 0.16 Å.[38] The effect of interplanar spacing on the charge transport characteristics of partially oxidized bisglyoximates will be explored further in the discussion of bisbenzoquinonedioximate systems.[7b] The relative insensitivity of conductivity to the metal has been noted in other highly conjugated, partially oxidized metal-macrocycle materials.[7a,8a,d]

A significant question in considering the conductivity increase brought about by $M(dpg)_2$ iodination is whether the charge transport path may not involve the stacked array of partially oxidized $M(dpg)_2$ units, but rather the chains of iodine atoms (as I_5^- units). Elemental iodine is a wide gap semiconductor which becomes metallic under sufficient pressure.[85] To explore this matter further, conductivity studies were undertaken on integral oxidation state materials with polyiodide chains. Polycrystalline samples of (trimesic acid·$H_2O)_{10}H^+I_5^-$ (having I_5^- chains[32]) exhibited electrical conductivity less than 10^{-7} $(\Omega\ cm)^{-1}$, while samples of (benzamide)$_2H^+I_3^-$ (having I_3^- chains[51]) were comparable in low conductivity: less than 10^{-8} $(\Omega\ cm)^{-1}$.[86] Experience indicates that for typical quasi-one-dimensional materials, polycrystalline samples will be ca. 10^{-2} less conductive than single crystals measured along the chain direction.[8a,b,87] Further evidence that the polyiodide chains play at most a minor role in charge transport is provided by results on the analogous brominated compounds. Both polycrystalline and single-crystal samples of the $M(dpg)_2Br$ materials display conductivities which are, within experimental error, nearly identical with those of the analogous $M(dpg)_2I$ materials.[59a] This demonstrates an insensitivity of the transport properties to the identity of the halogen. Similar conclusions have been reached in an organic system.[59b]

It is of interest to compare the facility of charge transport in the $M(dpg)_2I$ systems with that of other low-dimensional materials. To take account of differences in crystal structures, it is most meaningful to compare the mean free paths, L, which describe the average distance traveled by a charge carrier between scattering occurrences. From one-electron tight-binding band theory, the dc conductivity in the chain direction can be related to the mean free path by[86,88]

$$L = \frac{\pi h \sigma}{2e^2 N} \tag{11}$$

where N is the number of conducting chains per cross-sectional area. The mean free paths for the $M(dpg)_2I$ charge carriers are compared with those of several other stacked materials in Table XII. The parameters for the partially oxidized bisdiphenylglyoximates are comparable with those for "intermediate-conductivity" salts of TCNQ (tetracyanoquinodimethane).[89] The latter materials also exhibit temperature-dependent conductivity which follows eq 10.[89]

Table XII. Approximate Carrier Mean Free Paths for Some Stacked Conductors at 300 K[a]

material	mean free path, Å
$[(C_2H_5)_2TCC](TCNQ)_2$	2.3×10^{-6} [b]
$Ni(dpg)_2I$	2.0×10^{-3} to 4.0×10^{-4} [c]
$Pd(dpg)_2I$	8.0×10^{-5} to 1.3×10^{-5} [c]
$[(C_2H_5)_3NH](TCNQ)_2$	1.4×10^{-2} [d]
$Qn(TCNQ)_2$	0.43[e]
(TTF)(TCNQ)	2.3-3.5[f]
NiPcI	3.3-8.2[g]
TTF_2I_3	5.7-8.6[h]
Ni metal	60[i]

[a] Calculated from eq 11 using data from the sources indicated. [b] TCC = 3,3-diethylthiacarbocyaninium; Fedutin, D. N.; Shchegolev, I. F.; Stryukov, V. B.; Yagubskii, E. B.; Zvarykina, A. F.; Atovmyam, L. O.; Kaminski, V. F.; Shivaeva, R. P. *Phys. Status Solidi B*, **1971**, *48*, 87-92. [c] This work. [d] Reference 89 and Kobayashi, H.; Ohashi, Y.; Marumo, F.; Saito, Y. *Acta Crystallogr Sect. B* **1970**, *26*, 459-467. [e] Reference 89 and Kobayashi, H.; Marumo, F.; Saito, Y. *Acta Crystallogr., Sect. B.* **1971**, *27*, 373-378; Qn = quinolinium. [f] Reference 88b. [g] Reference 8b. [h] References 4c and 29b. [i] Reference 38.

The theoretical reasons for the observed temperature dependence of the electrical conductivity in quasi-one-dimensional stacked organic and metal-organic materials have been the subject of considerable discussion. For the $M(dpg)_2I$ compounds, which exhibit activated behavior with at most only minor leveling off of the conductivity at highest attainable temperatures, either of two currently proposed models appears to be applicable. Phonon-assisted hopping has been discussed for anisotropic systems in which the electronic states near the Fermi level are localized owing to static disorder.[88c,90] The lack of registry between polyiodide chains detected in the diffraction study is the most obvious structural disorder in the $M(dpg)_2I$ system. For the regime above the very lowest temperatures (where variable-range hopping occurs) this model predicts activated charge transport behavior, i.e., eq 10 is obeyed. At higher temperatures it is proposed that the electron-phonon interaction becomes stronger than the potential causing the localization, and the activated behavior is no longer observed. This higher temperature range is presumably beyond that which is practicable for the $M(dpg)_2I$ materials. Alternatively, a description has been put forward based on the observation that the conductivity of a number of low-dimensional materials can be fit to the equation[91]

$$\sigma = \sigma_0 T^{-\alpha} e^{-\Delta/kT} \tag{12}$$

Here α is a sample-dependent constant in the range of 3-4. It has been proposed that most of the electronic states in these materials are only weakly localized and that a band model with a gap (possibly a Mott-Hubbard gap or one associated with disorder-induced localization of states at the band edges) of 2Δ is applicable. The exponential term in eq 12 reflects an activated carrier concentration. The factor $T^{-\alpha}$ arises from a marked temperature dependence of the carrier mobility and can be related to coupling with molecular vibrations. In practice, a number of materials which conform to eq 12 exhibit a nearly linear region in the log σ vs. $1/T$ plot (although pronounced downward curvature is seen at higher temperatures). From the above discussion it can be seen that the relatively linear log σ vs. $1/T$ behavior of the $M(dpg)_2I$ materials is compatible with either conductivity model. A serious question

regarding the hopping picture is whether the disordered iodine chains could provide sufficient driving force for localization of the electronic wave functions in the $M(dpg)_2$ columns. A serious question with regard to the band model concerns the origin of the apparent gap. For the present case with a 90% filled band, it seems unlikely to be classical Mott-Hubbard in origin.[91b]

Conclusions

The results of this study demonstrate conclusively that $M(dpg)_2I$ compounds, M = Ni, Pd, contain the $M(dpg)_2$ units in formal fractional oxidation states, ca. +0.2. The accuracy of this number is limited primarily by the accuracy to which the stoichiometry of the compound is known and by the possible presence of small amounts of undetected iodine-containing species. A reasonable estimate of uncertainty is ±0.04 charge units. Thus, it is seen that the diffuse X-ray scattering, resonance Raman, and iodine-129 Mössbauer techniques are powerful complementary methods for polyiodide structure identification, and hence for direct measurement of charge distribution in mixed-valence structures. Judging from the $M(dpg)_2$ and other metallomacrocycle results,[7,8] the iodine oxidation procedure appears to have some efficacy in the synthesis of mixed-valence structures, and in the present case results both in shortening of the metal-metal distance (ca. 0.27 Å) and in dramatically increasing the c axis conductivity (ca. 10^7-10^8). Whether the charge carriers are transported through the chain of metal atoms as is likely in KCP ($K_2Pt(CN)_4Br_{0.3}\cdot 3H_2O$),[3b] or through the π systems of the ligand columns as in numerous organic conductors, has not been resolved. The large intermetal distances in the present case, i.e., 3.223 (3) Å (3.25 Å for Pd[14d]) vs. 2.89 Å in KCP,[92] and the relative insensitivity of the conductivity to the metal argue for the latter situation.[93]

It is reasonable to inquire whether chemical modification of the metal bisglyoximate core so as to allow greater conjugation and closer interplanar spacing will affect the degree of partial oxidation, transport properties, etc. This question is explored further in the accompanying article.[7b]

Acknowledgments. We thank Mr. C. B. Cooper for assistance with the 8 K Raman measurement. We are indebted to Professor J. B. Cohen for generously making his facilities for diffuse X-ray measurements available to us. This work was generously supported under the NSF-MRL program through the Materials Research Center of Northwestern University (Grant DMR76-80847), by the Office of Naval Research (T.J.M.), the Department of Energy (S.L.R.), and the National Science Foundation (Grant CHE76-10335 to J.A.I.).

Supplementary Material Available: A listing of structure amplitude tables (2 pages). Ordering information is given on any current masthead page.

References and Notes

(1) (a) Department of Chemistry and the Materials Research Center, Northwestern University. (b) Department of Electrical Engineering and the Materials Research Center, Northwestern University. (c) Physics Division, Argonne National Laboratory. (d) Thesis Parts Appointee, Argonne National Laboratory.
(2) (a) Fellow of the Alfred P. Sloan Foundation. (b) Camille and Henry Dreyfus Teacher-Scholar.
(3) (a) Devreese, J. T.; Evrard, R. P.; van Doren, V. E. "Highly Conducting One-Dimensional Solids", Plenum Press; New York, 1979. (b) Miller, J. S.; Epstein, A. J. *Ann. N.Y. Acad. Sci.*, **1978,** *313.* (c) Keller, H. J., Ed. "Chemistry and Physics of One-Dimensional Metals", Plenum Press: New York, 1977. (d) Miller, J. S.; Epstein, A. J. *Prog. Inorg. Chem.* **1976,** *20,* 1-151. (e) Keller, H. J., Ed. "Low Dimensional Cooperative Phenomena", Plenum Press: New York, 1975. (f) Soos, Z. G.; Klein In "Molecular Associations", Foster, R., Ed.; Academic Press: New York, 1975; Chapter 1. (g) Masuda, K.; Silver, M. "Charge and Energy Transfer in Organic Semiconductors", Plenum Press: New York, 1974. (h) Interrante, L. V. "Extended Interactions between Metal Ions in Transition Metal Complexes", ACS Symposium Series, No. 5, American Chemical Society: Washington, D.C., 1974. (i) Zeller, H. R. *Festkörperprobleme, 1973,* 13, 31-58.
(4) (a) Bloch, A. N.; Cowan, D. O.; Bechgaard, K.; Pyle, R. E.; Banks, R. H. *Phys. Rev. Lett.* **1975,** *34,* 1561-1564. (b) Ashwell, G. J.; Eley, D. D.; Willis, M. R. *Nature (London)* **1976,** *259,* 201-202. (c) Isett, L. C.; Perez-Albuerne, E. A. *Solid State Commun.* **1977,** *21,* 433-435. (d) Bechgaard, K.; Jacobsen, C. S.; Anderson, N. H. *ibid.* **1978,** *25,* 875-879.
(5) (a) Garito, A. F.; Heeger, A. J. *Acc. Chem. Res.* **1974,** *7,* 232-240. (b) Haddon, R. C. *Nature (London)* **1975,** *256,* 394-396. (c) Soos, Z. G. *Annu. Rev. Phys. Chem.* **1974,** *25,* 121-153.
(6) (a) Pouget, J. P.; Khanna, S. K.; Denoyer, F.; Comes, R.; Garito, A. F.; Heeger, A. J. *Phys. Rev. Lett.* **1976,** *37,* 437-440. (b) Torrance, J. B.; Scott, B. A.; Kaufman, F. B. *Solid State Commun.* **1975,** *17,* 1369-1373. (c) Butler, M. A.; Wudl, F.; Soos, Z. G. *Phys. Rev. B* **1975,** *12,* 4708-4719. (d) LaPlaca, S. J.; Corfield, P. W. R.; Thomas, R.; Scott, B. A. *Solid State Commun.* **1975,** *17,* 635-638. (e) Coppens, P. *Phys. Rev. Lett.* **1975,** *35,* 98-100. (f) Torrance, J. B. *Acc. Chem. Res.*, **1979,** *12,* 79-86. (g) Torrance, J. B. *Ann. N.Y. Acad. Sci.* **1978,** *313,* 210-232. (h) For apparent exceptions to this generalization, involving second- and third-row transition metal ions, see Reise, A. H., Jr.; Hagley, V. S.; Petersen, S. W. *J. Am. Chem. Soc.* **1977,** *99,* 4184-4186. Gordon, J. G., II; Williams, R.; Hsu, C.-H.; Cuellar, E.; Samson, S.; Mann, K.; Gray, H. B.; Hadek, V.; Somoano, R. *Ann. N.Y. Acad. Sci.* **1978,** *313,* 580-593.
(7) (a) Marks, T. J. *Ann. N.Y. Acad. Sci.* **1978,** *313,* 594-616. (b) Brown, L. D.; Kalina, D. W.; McClure, M. S.; Ruby, S. L.; Schultz, S.; Ibers, J. A.; Kannewurf, C. R.; Marks, T. J. *J. Am. Chem. Soc.*, following paper in this issue. (c) Gleizes, A.; Marks, T. J.; Ibers, J. A. *ibid.* **1975,** *97,* 3545-3546. (d) Marks, T. J.; Gleizes, A.; Ibers, J. A. "Abstracts of Papers", 170th National Meeting of the American Chemical Society, Chicago, Ill., Aug 1975; American Chemical Society: Washington, D.C., 1975; INOR 54.
(8) (a) Petersen, J. L.; Schramm, C. S.; Stojakovic, D. R.; Hoffman, B. M.; Marks, T. J. *J. Am. Chem. Soc.* **1977,** *99,* 286-288. (b) Schramm, C. S.; Stojakovic, D. R.; Hoffman, B. M.; Marks, T. J. *Science* **1978,** *200,* 47-48. (c) Peterson, J. L.; Schramm, C. S.; Scaringe, R. P.; Stojakovic, D. R.; Hoffman, B. M.; Ibers, J. A.; Marks, T. J., manuscript in preparation. (d) Lin, L.-S.; Marks, T. J., submitted for publication.
(9) (a) Popov, A. I. *MTP Int. Rev. Sci.: Inorg. Chem., Ser. One* **1972,** *3.* (b) Huheey, J. H., "Inorganic Chemistry", 2nd Ed., Harper and Row: New York, 1978, pp 666-669.
(10) (a) Marks, T. J.; Webster, D. F.; Ruby, S. L.; Schultz, S. *J. Chem. Soc., Chem. Commun.* **1976,** 444-445. (b) Teitelbaum, R. C.; Ruby, S. L.; Marks, T. J. *J. Am. Chem. Soc.* **1978,** *100,* 3215-3217. (c) Kalina, D. W.; Stojakovic, D. R.; Teitelbaum, R. C.; Marks, T. J., manuscript in preparation.
(11) Williams, D. E.; Wohlauer, G.; Rundle, R. E. *J. Am. Chem. Soc.* **1959,** *81,* 755-756.
(12) Edelman, L. E. *J. Am. Chem. Soc.* **1950,** *72,* 5765-5766.
(13) Underhill, A. E.; Watkins, D. M.; Pethig, R. *Inorg. Nucl. Chem. Lett.* **1973,** *9,* 1269-1273.
(14) (a) Miller, J. S.; Griffiths, C. H. *J. Am. Chem. Soc.* **1977,** *99,* 749-755. (b) Mehne, L. F.; Wayland, B. B. *Inorg. Chem.* **1975,** *14,* 881-885. (c) Keller, H. J.; Seibold, K. *J. Am. Chem. Soc.* **1971,** *93,* 1309-1310. (d) Foust, A. S.; Soderberg, R. *ibid.* **1967,** *89,* 5507-5508.
(15) (a) Foster, R. "Organic Charge-Transfer Complexes", Academic Press: New York, 1969. (b) Mulliken, R. S.; Person, W. B. "Molecular Complexes", Wiley-Interscience: New York, 1969.
(16) (a) Barefield, E. K.; Mocella, M. T. *J. Am. Chem. Soc.* **1975,** *97,* 4238-4246. (b) Lovecchio, F. V.; Gore, E. S.; Busch, D. H. *ibid.* **1974,** *96,* 3109-3118. (c) Dolphin, D.; Niem, T.; Felton, R. H.; Fujita, I. *ibid.* **1975,** *97,* 5288-5290. (d) Lappin, A. G.; Murray, C. K.; Margerum, D. W. *Inorg. Chem.* **1978,** *17,* 1630-1634, and references cited therein. (e) Johnson, E. C.; Niem, T.; Dolphin, D. *Can. J. Chem.* **1978,** *56,* 1381-1388.
(17) Cooper, C. B. Ph.D. Thesis, Northwestern University, July 1978.
(18) (a) The program GENFIT was written at Argonne National Laboratory by Dr. B. J. Zabransky and modified by R. C. Teitelbaum. It is based on the nonlinear least-squares minimization method of Powell.[18b] (b) Powell, M. J. D. *Comput. J.* **1965,** *7,* 303-307.
(19) (a) Ruby, S. L. "Mössbauer Effect Methodology", Vol. 8; 1973; pp 263-276. (b) The traditional goodness-of-fit parameter

$$\chi^2 = \sum_i^n [(\chi_i - \chi_{ic})/\Delta\chi_i]^2$$

gives satisfactorily small values for either a good model (the calculated values χ_{ic} agree well with the data χ_i) or for a poor experiment ($\Delta\chi_i$ is large).[18]
(20) Schafer, D. E.; Wudl, F.; Thomas, G. A.; Ferraris, J. P.; Cowan, D. D. *Solid State Commun.* **1974,** *14,* 347-351.
(21) We thank Dr. R. Bastasz for a copy of this program.
(22) Cowie, M.; Ibers, J. A. *Inorg. Chem.* **1976,** *15,* 552-557.
(23) Doedens, R. J.; Ibers, J. A. *Inorg. Chem.* **1967,** *6,* 204-210.
(24) The Northwestern absorption program, AGNOST, includes the Coppens-Leiserowitz-Rabinovitch logic for Gaussian integration. The diffractometer was run under the disc oriented Vanderbilt system (Lenhert, P. G. *J. Appl. Crystallogr.* **1975,** *8,* 568-570). Other programs used are described in ref 22.
(25) For nonhydrogen atom scattering factors see Cromer, D. T.; Waber, J. T. "International Tables for X-ray Crystallography", Vol. IV; Kynoch Press: Birmingham, England, 1974; Table 2.2A. For hydrogen atoms see Stewart, R. F.; Davidson, E. R.; Simpson, W. T. *J. Chem. Phys.* **1965,** *42,* 3175-3187.
(26) Cromer, D. T.; Liberman, D. *J. Chem. Phys.* **1970,** *53,* 1891-1898.
(27) Warren, B. E. "X-ray Diffraction", Addison-Wesley: Reading, Mass., 1969; p 35.
(28) Scaringe, R. P.; Ibers, J. A. Unpublished results.
(29) See paragraph at end of paper regarding supplementary material.
(30) (a) Endres, H.; Keller, H. J.; Mégnamisi-Bélombé, M.; Moroni, W.; Pritzkow, H.; Weiss, J.; Comes, R. *Acta Crystallogr., Sect. A* **1976,** *32,* 954-957. (b) Smith, D. L.; Luss, H. R. *Acta Crystallogr., Sect. B* **1977,** *33,* 1744-1749. (c) Huml, K. *Acta Crystallogr.* **1967,** *22,* 29-32.

(31) Beyeler, H. U. *Phys. Rev. Lett.* **1976,** *37*, 1557–1560.
(32) (a) Chains of linear I_5^- ions are found in (trimesic acid·H_2O)$_{10}H^+I_5^-$. See Herbstein, F. H.; Kapon, M. *Acta Crystallogr., Sect. A* **1972,** *28*, S74, and private communication to T.J.M. (b) The structures of all known polyiodides[9] can be understood in terms of various groupings of I^-, I_2, and I_3^- units.[9b] Thus, I_5^- consists of an I^- ion symmetrically disposed between two I_2 units.
(33) Endres, H.; Keller, H. J.; Moroni, W.; Weiss, J. *Acta Crystallogr., Sect. B* **1975,** *31*, 2357–2358.
(34) Robertson, J. M.; Woodward, I. *J. Chem. Soc.* **1937,** 219–220.
(35) (a) Millar, M.; Holm. R. H. *J. Am. Chem. Soc.* **1975,** *97*, 6052–6058. (b) Peng, S.-M.; Ibers, J. A.; Millar, M.; Holm, R. H. *ibid.* **1976,** *98*, 8037–8041.
(36) Peng, S.-M.; Goedken, V. L. *J. Am. Chem. Soc.* **1976,** *98*, 8500–8510.
(37) Charlson, A. J.; Stephens, F. S.; Vagg, R. S.; Watton, E. C. *Inorg. Chim. Acta* **1977,** *25*, L51–L52.
(38) (a) Handbook of Chemistry and Physics", 57th ed.; Chemical Rubber Publishing Co.: Cleveland, Ohio, 1976–1977; p F-216. (b) Shannon, R. D. *Acta Crystallogr., Sect. A* **1976,** *32*, 751–767.
(39) Sacconi, L. *Transition Met. Chem.* **1968,** *4*, 199–298.
(40) Fleischer, E. B. *J. Am. Chem. Soc.* **1963,** *85*, 146–148.
(41) Hamor, T. A.; Caughey, W. S.; Hoard, J. L. *J. Am. Chem. Soc.* **1965,** *87*, 2305–2312.
(42) (a) Meyer, E. F., Jr. *Acta Crystallogr., Sect. B* **1972,** *28*, 2162–2167. (b) Cullen, D. L.; Meyer, E. F., Jr. *J. Am. Chem. Soc.* **1974,** *96*, 2095–2102.
(43) Dwyer, P. N.; Buchler, J. W.; Scheidt, W. R. *J. Am. Chem. Soc.* **1974,** *96*, 2789–2795.
(44) See, for example, Guinier, A. "X-ray Diffraction in Crystals, Imperfect Crystals, and Amorphous Bodies", W. H. Freeman: San Francisco, 1963; p 154.
(45) (a) Johnson, B. B.; Peticolas, W. L. *Annu. Rev. Phys. Chem.* **1976,** *27*, 465–491. (b) Warshel, A. *Annu. Rev. Biophys. Bioeng.* **1977,** *6*, 273–300. (c) Spiro, T. G. "Chemical and Biochemical Applications of Lasers", Moore, C. B., Ed.; Academic Press: New York, 1974; Chapter 2. (d) Tang, J.; Albrecht, A. C. "Raman Spectroscopy", Vol. 2; Szymanski, H. A., Ed.; Plenum Press: New York, 1970; Chapter 2.
(46) (a) Johnson, B. B.; Nafie, L. A.; Peticholas, W. L. *Chem. Phys.* **1977,** *19*, 303–311. (b) Nafie, L. A.; Pastor, R. W.; Dobrowiak, J. C.; Woodruff, W. H. *J. Am. Chem. Soc.* **1976,** *98*, 8007–8014. (c) Stein, P.; Miskowski, V.; Woodruff, W. H.; Griffin, J. P.; Werner, K. G.; Gaber, B. P.; Spiro, T. G. *J. Chem. Phys.* **1976,** *64*, 2159–2167. (d) Mingardi, M.; Siebrand, W. *ibid.* **1975,** *62*, 1074–1085.
(47) Kiefer, W. *Appl. Spectrosc.* **1974,** *28*, 115–133.
(48) Runsink, J.; Swen-Walstra, S.; Migchelsen, T. *Acta. Crystallogr., Sect. B* **1972,** *28*, 1331–1335.
(49) (a) Maki, A. G.; Forneris, R. *Spectrochim. Acta, Part A* **1967,** *23*, 867–880, and references cited therein. (b) Haywood, G. C.; Hendra, P. J. *ibid.* **1967,** *23*, 2309–2314.
(50) (a) Gabes, W.; Nijman-Meester, M.A.M. *Inorg. Chem.* **1973,** *12*, 589–592. (b) Datta, S. N.; Ewig, C. S.; Van Wazer, J. R. *J. Mol. Struct.* **1978,** *48*, 407–416.
(51) Reddy, J. M.; Knox, K.; Robin, M. B. *J. Chem. Phys.* **1964,** *40*, 1082–1089.
(52) A number of highly conductive organic materials display a similar structural motif of stacks and I_3^- chains. See, for example, ref 30b,c and Delhaes, P.; Cougrand, A.; Flandrois, S.; Chasseau, D.; Gaultier, J.; Hauw, C.; Dupuis, P. *Lect. Notes Phys.* **1977,** *65*, 493–498.
(53) (a) Brown, R. D.; Nunn, E. K. *Aust. J. Chem.* **1966,** *19*, 1567–1576. (b) Migchelsen, T.; Vos, A. *Acta Crystallogr.* **1967,** *22*, 812–815. (c) Rundle, R. E. *ibid.* **1961,** *14*, 585–589.
(54) (a) Correlation field effects are generally observed to be relatively small in polyiodides.[10c] For example, the factor group splitting in solid I_2 is only ca. 8 cm^{-1}.[55b] (b) Anderson, A.; Sun, R. S. *Chem. Phys. Lett.* **1970,** *6*, 611–616.
(55) (a) Havinga, E. E.; Boswijk, K. H.; Wiebenga, E. H. *Acta Crystallogr.* **1954,** *7*, 487–490. (b) Herbstein, F. H.; Kapon, M. *Nature (London)* **1972,** *239*, 153–154. (c) Havinga, E. E.; Wiebenga, E. H. *Acta Crystallogr.* **1958,** *11*, 733–737.
(56) Hach, R. J.; Rundle, R. E. *J. Am. Chem. Soc.* **1951,** *73*, 4321–4324.
(57) Since this normal mode has the same symmetry (A_{1g} under $D_{\infty h}$) as the 160-cm^{-1} mode, there is presumably some mixing of the vibrations.
(58) (a) Gabes, W.; Stufkens, D. J. *Spectrochim. Acta, Part A* **1974,** *30*, 1835–1841, and references cited therein. (b) Robin, M. B. *J. Chem. Phys.* **1964,** *40*, 3369–3377.
(59) (a) Kalina, D. W.; McClure, M. S.; Kannewurf, C. R.; Marks, T. J., manuscript in preparation. (b) Kamarás, K.; Mihaly, G.; Grüner, G.; Jánossy, A. *J. Chem. Soc., Chem. Commun.* **1978,** 974–975.
(60) (a) Sunder, S.; Mendelsohn, R.; Bernstein, H. J. *J. Chem. Phys.* **1975,** *63*, 573–580. (b) Friedman, J. M.; Hochstrasser, R. M. *J. Am. Chem. Soc.* **1976,** *98*, 4043–4048. (c) Shelnutt, J. A.; O'Shea, D. C.; Yu, N.-T.; Cheung, L. D.; Felton, R. H. *J. Chem. Phys.* **1976,** *64*, 1156–1165.
(61) Woodruff, W. M.; Pastor, R. W.; Dobrowiak, J. C. *J. Am. Chem. Soc.* **1976,** *98*, 7999–8006.
(62) (a) Gibb, T. C. "Principles of Mössbuaer Spectroscopy", Chapman and Hall: London, 1976; Chapter 4.2. (b) Bancroft, G. M.; Platt, R. H. *Adv. Inorg. Chem. Radiochem.* **1972,** *15*, 59–258.
(63) Data for Ni(dpg)$_2$I and Pd(dpg)$_2$I have been averaged.
(64) (a) Potasek, M. J.; Debrunner, P. G.; Morrison, W. H., Jr.; Hendrickson, D. N. *J. Chem. Phys.* **1974,** *60*, 2203–2206. (b) Ehrlich, B. S.; Kaplan, M. *ibid.* **1969,** *51*, 603–606. (c) deWaard, H.; Ruby, S. L.; Teitelbaum, R. C. Unpublished results on $Cs^{129}I_3$.
(65) (a) Lucken, E. A. C. "Nuclear Quadrupole Coupling Constants", Academic Press: New York, 1969; Chapter 1. (b) Dailey, B. P.; Townes, C. H. *J. Chem. Phys.* **1955,** *23*, 118–123. (c) Ruby, S. L.; Shenoy, G. K. "Mössbauer Isomer Shifts", Shenoy, G. K.; Wagner, F. E., Eds., North-Holland Publishing Co.: Amsterdam, 1978; Chapter 9b.
(66) (a) Bukshpan, S.; Goldstein, C.; Sonnino, T.; May, L.; Pasternak, M. *J. Chem. Phys.* **1975,** *62*, 2606–2609. (b) deWaard, H. "Mössbauer Effect Data Index", 1973; pp 447–494. (c) This means that for a similar class of compounds, there will be a linear relationship between δ and e^2qQ.
(67) That the sum of the charges on each ion does not equal −1.0 illustrates the qualitative nature of this approach.
(68) The charge on the central iodine atoms of the I_3^- groups in $Ru(C_5H_5)_2I^+I_3^-$ and $(C_6H_5CONH_2)_2H^+I_3^-$, calculated from the published isomer shifts, is not in optimal agreement, so both values are given.
(69) (a) Anex, B. G. *ACS Symposium Series*, No. 5, American Chemical Society; Washington, D.C., 1974; pp 276–300. (b) Hara, Y.; Shirotani, I.; Onodera, A. *Solid State Commun.* **1976,** *19*, 171–175. (c) Ohashi, Y.; Hanazaki, I.; Nagakura, S. *Inorg. Chem.* **1970,** *9*, 2551–2556.
(70) (a) Anex, B. G.; Krist, F. K. *J. Am. Chem. Soc.* **1967,** *89*, 6114–6125. (b) Banks, C. V.; Barnum, D. W. *ibid.* **1958,** *80*, 4767–4772.
(71) Basu, G.; Cook, G. M.; Belford, R. L. *Inorg. Chem.* **1964,** *3*, 1361–1368.
(72) Zahner, J. C.; Drickamer, H. G. *J. Chem. Phys.* **1960,** *33*, 625–1628.
(73) (a) Day, P. In ref 3c, p 191. (b) Beattie, J. K.; Hush, N. S.; Taylor, P. R. *Inorg. Chem.* **1976,** *15*, 992–993. (c) Hush, N. S. *Prog. Inorg. Chem.* **1967,** *8*, 391–444. (d) Robin, M. B.; Day, P. *Adv. Inorg. Chem. Radiochem.* **1967,** *10*, 247–422. (e) The thermal parameters in the Ni(dpg)$_2$ portion of the Ni(dpg)$_2$I low-temperature structure gave no evidence of metrically nonequivalent sites, which might arise in a trapped valence situation.
(74) Stojakovic, D. R. Ph.D. Thesis, Northwestern University, Evanston, Ill., Aug 1977.
(75) Such studies are in progress.
(76) (a) Swingle, R. S., II; Riggs, W. M. *Crit. Rev. Anal. Chem.* **1975,** *5*, 267–321. (b) Jolly, W. L. *Top. Curr. Chem.* **1977,** *71*, 149–182. (c) *Coord. Chem. Rev.* **1974,** *13*, 47–81. (d) Hercules, D. M.; Carver, J. C. *Anal. Chem.* **1974,** *46*, 133R–150R.
(77) (a) Cowan, D. O.; Park, J.; Barber, M.; Swift, P. *Chem. Commun.* **1971,** 1444–1446. (b) Cahen, D.; Lester, J. E. *Chem. Phys. Lett.* **1973,** *18*, 108–111. (c) Burroughs, P.; Hammett, A.; Orchard, A. F. *J. Chem. Soc., Dalton Trans.* **1974,** 565–567. (d) Thomas, J. M.; Tricker, M. J. *J. Chem. Soc., Faraday Trans. 2* **1975,** 329–336. (e) Helmer, J. E. *J. Electron Spectrosc. Relat. Phenom.* **1973,** *1*, 259–267. (f) Oku, M.; Hirokawa, K. *J. Electron. Spectrosc. Relat. Phenom.* **1976,** *8*, 475–481.
(78) Orchard, A. F.; Thornton, G. *J. Chem. Soc., Dalton Trans.* **1977,** 1238–1240.
(79) Hush, N. S. *Chem. Phys.* **1975,** *10*, 361–366.
(80) Matienzo, L. J.; Yin, L. I.; Grim, S. O.; Swartz, W. D. *Inorg. Chem.* **1973,** *12*, 2762–2769.
(81) (a) Kumar, G.; Blackburn, J. R.; Albridge, R. G.; Moddeman, W. E.; Jones, M. M. *Inorg. Chem.* **1972,** *11*, 296–300. (b) Clark, D. T.; Adams, D. B. *Chem. Commun.* **1971,** 602–604.
(82) Hedman, Jr.; Klasson, M.; Nilsson, R.; Nordling, C.; Sorokina, M. F.; Kljushnikov, O. I.; Nemnonov, S. A.; Trapeznikov, V. A.; Zyryanov, V. G. *Phys. Scr.* **1971,** *4*, 195–201.
(83) (a) Lin, L. I.; Ghose, S.; Alder, I. *Appl. Spectrosc.* **1972,** *26*, 355–357. (b) Kim, K. S.; Baitinger, W. E.; Amy, J. W.; Winograd, N. J. *J. Electron Spectrosc. Relat. Phenom.* **1974,** *5*, 351–357.
(84) Such behavior is observed for the more conductive, partially oxidized phthalocyanines.[8b]
(85) Riggleman, B. M.; Drickamer, H. G. *J. Chem. Phys.* **1963,** *38*, 2721–2724.
(86) Jacobsen, C. S.; Mortensen, K.; Andersen, J. R.; Bechgaard, K. *Phys. Rev. B* **1978,** *18*, 905–921.
(87) See, for example, Wheland, R. C.; Gillson, J. L. *J. Am. Chem. Soc.* **1976,** *98*, 3916–3925. Chiang, C. K.; Druy, M. A.; Gau, S. C.; Heeger, A. J.; Louis, E. J.; MacDiarmid, A. G.; Park, Y. W.; Shirakawa, H. *ibid.* **1978,** *100*, 1013–1015.
(88) (a) Berlinsky, A. J. *Contemp. Phys.* **1976,** *17*, 331–354. (b) Thomas, G. A., et al. *Phys. Rev. B* **1976,** *13*, 5105–5110. (c) Bloch, A. N.; Welsman, R. B.; Varma, C. M. *Phys. Rev. Lett.* **1972,** *28*, 753–756.
(89) Shchegolev, I. F. *Phys. Status Solidi A* **1972,** *12*, 9–45.
(90) (a) Shante, V. K. S. *Phys. Rev. B* **1977,** *16*, 2597–2612, and references cited therein. (b) Cohen, M. H. *Lect. Notes Phys.* **1977,** *65*, 225–265, and references cited therein. (c) Mihály, G.; Ritvay-Emandity, K.; Jánossy, A.; Holczer, K.; Grüner, G. *Solid State Commun.* **1977,** *21*, 721–724. (d) Mott, N. F. "Metal-Insulator Transitions", Taylor and Francis: London, 1974; Chapter 1.7.
(91) (a) Epstein, A. J.; Conwell, E. M.; Sandman, D. J.; Miller, J. S. *Solid State Commun.* **1977,** *23*, 335–358. (b) Epstein, A. J.; Conwell, E. M. *Ibid.* **1977,** *24*, 627–630. (c) Conwell, E. M. *Phys. Rev. Lett.* **1977,** *39*, 777–780.
(92) Williams, J. M.; Petersen, J. L.; Gerdes, H. M.; Peterson, S. W. *Phys. Rev. Lett.* **1974,** *33*, 1079–1081.
(93) Although the observation of a ligand-centered free radical in the EPR spectrum also supports this conclusion, the fact that very pure samples exhibit no signal renders this observation somewhat less meaningful.[14b]